

## Young Scientists Summer Program

# Towards harnessing uncertainty of ecological network indicators in ecosystem management

Gemma Gerber

*gemmagerber@live.com*

---

### Approved by:

**Mentors:** Elena Rovenskaya, Brian Fath, Ursula Scharler

**Program:** Advancing Systems Analysis (ASA)

**Date:** 29 September 2022

This report represents the work completed by the author during the IIASA Young Scientists Summer Program (YSSP) with approval from the YSSP mentors.

It was finished by **29 September 2022** and has not been altered or revised since.

### Mentor signature(s):

---

Elena Rovenskaya

---

Brian Fath

---

Ursula Scharler

---

## Table of contents

Abstract.....	4
About the author.....	5
Acknowledgments .....	5
1 Introduction .....	6
1.1 Background .....	6
1.2 Aims & Objectives .....	7
2 Methods .....	8
2.1 Case study site .....	8
2.2 Data collection & food web model construction .....	9
2.3 Solving food web network solutions .....	10
2.3.1 Single food web solutions .....	10
2.3.2 Ensemble food web solutions .....	10
2.4 Ecological Network Analysis .....	11
2.5 Statistical Analysis.....	12
2.5.1 Pairwise relationships .....	12
2.5.2 Comparison of ensembles .....	12
3 Results .....	13
3.1 Comparing network properties from single & ensemble solutions .....	13
3.1.1 Flows.....	13
3.1.2 Ecological Indicators.....	13
3.2 Frequency of extreme values calculated from single network solutions .....	16
3.3 Pairwise relationships between ecologically related flows.....	19
3.4 Pairwise relationships between ecologically related indicators .....	23
3.5 uMdloti Estuary temporal ecosystem function .....	24
3.5.1 System-level function .....	24
3.5.2 Node-level function .....	27
4 Discussion.....	30
4.1 Can ensemble solutions provide more robust estimates of ecosystem function than single solutions? .....	30
4.1.1 Ecological indicators derived from single network solutions .....	30
4.1.2 Ecological indicators derived from ensemble network solutions.....	31
4.2 Temporal comparison of uMdloti ecosystem function .....	32
4.3 Limitations of ensemble methods in ecological modelling .....	34
4.3.1 LIM-MCMC algorithm parameter selection .....	34
4.3.2 LIM-MCMC Sampling Adequacy .....	36
5 Conclusions.....	37
References .....	38
Supplementary Information 1 .....	41
Supplementary Information 2 .....	42
Supplementary Information 3 .....	43
Supplementary Information 4 .....	45

---

## ZVR 524808900

Disclaimer, funding acknowledgment, and copyright information:

*IIASA Reports* report on research carried out at IIASA and have received only limited review. Views or opinions expressed herein do not necessarily represent those of the institute, its National Member Organizations, or other organizations supporting the work.

### UPDATE OR DELETE

For *IIASA Working Papers/Reports/Policy Briefs funded by the IIASA core budget* we ask the authors to include the following:

The authors gratefully acknowledge funding from IIASA and the National Member Organizations that support the institute (The Austrian Academy of Sciences; The Brazilian Federal Agency for Support and Evaluation of Graduate Education (CAPES); The National Natural Science Foundation of China (NSFC); The Academy of Scientific Research and Technology (ASRT), Egypt; The Finnish Committee for IIASA; The Association for the Advancement of IIASA, Germany; The Technology Information, Forecasting and Assessment Council (TIFAC), India; The Indonesian National Committee for IIASA; The Iran National Science Foundation (INSF); The Israel Committee for IIASA; The Japan Committee for IIASA; The National Research Foundation of Korea (NRF); The Mexican National Committee for IIASA; The Research Council of Norway (RCN); The Russian Academy of Sciences (RAS); Ministry of Education, Science, Research and Sport, Slovakia; The National Research Foundation (NRF), South Africa; The Swedish Research Council for Environment, Agricultural Sciences and Spatial Planning (FORMAS); The Ukrainian Academy of Sciences; The Research Councils of the UK; The National Academy of Sciences (NAS), USA; The Vietnam Academy of Science and Technology (VAST).

For research funded by an external third party we ask the authors to include the full name of the funder, the title of the project and the grant number, e.g. The authors gratefully acknowledge funding from the European Research Council for the research project 'Forecasting Societies Adaptive Capacities to Climate Change' (FUTURESOC, FP7 230195).



This work is licensed under a [Creative Commons Attribution-NonCommercial 4.0 International License](#).  
For any commercial use please contact [permissions@iiasa.ac.at](mailto:permissions@iiasa.ac.at)

## Abstract

1. Ecosystem goods and services are dependent on the overall functioning of the ecosystem within naturally variable environmental conditions. Ecosystem function can be investigated through food web models describing the flows of energy/material (interactions) between species or functional groups. The impracticality of empirically measuring every food web flow can be addressed through linear inverse modelling (LIM), which estimates one solved food web from ecologically derived flow inequalities. Thereafter, Ecological Network Analysis (ENA) is applied to the solved food web to calculate ecological indicators describing ecosystem-level function. However, ecological indicators calculated on single food web solutions may not be representative of the actual system's functional variability.
2. Ecosystem modelling has evolved to incorporate ecological data variability through solving ensembles of plausible food webs using LIM coupled with Markov Chain Monte Carlo (LIM-MCMC) techniques, introducing uncertainty of ecosystem function. Using food web ensembles and ecological indicators of a case study ecosystem, we aimed to 1) explore the differences in ecosystem network properties derived from single solution food webs and ensembles of plausible food webs, and 2) investigate if ensemble methods can provide more robust estimates of ecosystem function than single solution methods.
3. We constructed thirteen monthly food web models (2015 – 2016) of uMdloti Estuary, South Africa, to serve as a basis for our investigation. Flow values were parametrised with ecologically derived inequalities, reflecting the empirical ecological variability within the system. We used three LIM algorithms commonly accepted by ecologists to calculate single network solutions for each model. We complemented the single solutions with ensembles of 10,000 plausible network solutions solved using LIM-MCMC. We then applied Ecological Network Analysis (ENA) to all solved networks.
4. We found that ecological indicators calculated from single network solutions were often underestimates of ensembles, potentially limiting realistic ecological inferences. In contrast, ensemble solutions have the benefit of 1) incorporating ecological variability in ecosystem models, offering more robust estimates of ecosystem function, and 2) detecting shifts in ecosystem states after disturbance events. Using ensemble solutions, we found that uMdloti ecosystem displays a reliance on primary producers to fuel the food web, low cycling of material/energy, and seasonal patterns of increased system activity during summer months. When we consider these ecological interpretations together, we can infer that uMdloti ecosystem shows a decreased capacity to maintain system function during drought conditions and is potentially more vulnerable to further perturbations affecting ecosystem function.
5. From an ecosystem management perspective, more robust inferences of ecosystem status through ensemble methods, together with the advantage of statistical comparisons, may enhance data-driven decision making and contribute toward good ecosystem management practices. The next steps of this research are to investigate the communication of ensemble uncertainty in a practical and meaningful way for inclusion in ecosystem assessments and management. As ecosystem properties cannot be directly managed, connecting ecosystem-level information to nodal information can provide insight into how the system components (nodes) can be managed in a way to improve overall system function. The next steps of this research are to investigate which indicators may be most meaningful to managers trying to maintain the flow of ecosystem services.

**Keywords:** food webs, ecological variability, uncertainty, estuarine management, linear inverse modelling, ecological network analysis, ensemble models

## About the author

**Gemma Gerber** is a PhD Candidate at the School of Life Sciences, University of KwaZulu-Natal, South Africa  
(Contact: [gemmagerber@live.com](mailto:gemmagerber@live.com))

## Acknowledgments

The research was developed at the Young Scientists Summer Program (YSSP) at the International Institute for Applied Systems Analysis (IIASA), Laxenburg, Austria, with financial support from the National Research Foundation (NRF) of South Africa.

# 1 Introduction

---

## 1.1 Background

One way to value ecosystems is through their high biological productivity to maintain ecological and socio-economic goods and services (Day and Rybczyk, 2019). The provision of these goods and services is dependent on the overall functioning of the system within the limits of natural variability (physical, chemical, and biological) (Mukherjee et al., 2019). Global change, resulting from anthropogenic activities and changes in climate drivers due to accelerated global warming, is predicted to alter the natural variability of environmental conditions experienced by ecosystems (Chevillot et al., 2018; Day and Rybczyk, 2019). The alteration of the natural variability of environmental conditions threatens the productivity of ecosystems by changing the balance of human impacts and ecosystem fundamental properties and overall functioning (Chevillot et al., 2018). To maintain ecosystem function under global change conditions, there is an urgent need for appropriate monitoring, management, and conservation strategies to protect the provision of ecosystem goods and services in future.

An important step in the development of ecosystem management and conservation strategies is the assessment of overall function of the ecosystem in question. Holistic approaches to understand ecosystem function often involve exploring food webs to identify ecosystem-level emergent properties (D'Alelio et al., 2016; Jørgensen and Fath, 2006). Conceptually, food webs are maps of trophic connections between species or functional groups ('nodes'), where trophic connections serve as energy 'flows' between nodes (Fath et al., 2007; Scharler and Borrett, 2021). Ecological Network Analysis (ENA) can be applied to food webs to calculate ecological indicators based on the direct and indirect energy interactions within the food webs (de Jonge and Schückel, 2021; Lau et al., 2017). The ENA indicators calculated on the food web are extrapolated to characterise emergent whole-system properties, such as functioning, providing useful insight into otherwise unmeasurable emergent system properties.

The first challenge in food web modelling is the conceptualisation and quantification of food webs. Given the inherent complexity of empirical food webs and the difficulty of estimating flow values from direct measurements, the empirical input data are often insufficient to quantify all flows in the food web (Kones et al., 2009; Soetaert and van Oevelen, 2009). There are typically more unknown flow values than quantified flows in food web models, resulting in a state of 'under-determinacy' (Kones et al., 2009; Soetaert and van Oevelen, 2009; Van den Meersche et al., 2009; van Oevelen et al., 2010). In under-determined networks, there exists an infinite number of plausible flow solutions, from which one plausible solution can be estimated through linear inverse modelling (LIM) methods.

Linear Inverse Modelling (LIM) describes the food web model as a linear mathematical function of the flows (van Oevelen et al., 2010). LIM uses the observed input data as linear equations to define a polytope of solution in Euclidean space ('solution space'), with each linear equation defining a boundary of the solution space. Flow inequalities (i.e., constraints) representative of the empirical observations introduces uncertainty in the model (van Oevelen et al., 2010; Waspe et al., 2018). Within the solution space, an infinite number of plausible food web configurations exist (Soetaert and van Oevelen, 2009; Van den Meersche et al., 2009; van Oevelen et al.,

2010). From these plausible food web configurations, a single solved configuration can be estimated using established LIM algorithms such as the central solution (Soetaert et al., 2009), parsimonious solution (flow vector that has the smallest sum of squared values) (Kones et al., 2009; Vézina and Platt, 1988) and likelihood-approach solutions (van Oevelen et al., 2010). The single solution returns one solved (i.e., plausible) food web model, where each flow value in the food web model has been estimated from several plausible flow values within the solution space. Solved flow values are thereafter analysed with ENA, which calculates various mathematical indicators that can be used to describe characterise ecosystem function.

A potential problem with empirically derived single network solutions is that they only capture a snapshot of potential ecosystem function. Therefore, one plausible food web configuration does not represent the range of potential ecosystem energy flows, limiting the ecological relevance of this method (Scharler and Borrett, 2021; Soetaert and van Oevelen, 2009). The focus of this research is how to capture ecological variability and quantify uncertainty in ecosystem function into useful indicators for ecosystem management.

To address some the constraints with single solution methods, a recent approach is to look at not one realization of the network model, but to solve ensembles of multiple plausible solutions from the solution space. The ensembles are sampled from the solution space using iterative Markov Chain Monte Carlo (MCMC) random walk algorithms (collectively referred to as LIM-MCMC) (Kones et al., 2006; Van den Meersche et al., 2009; van Oevelen et al., 2010). Each plausible solution within the ensemble is a valid and unique configuration of the food web flows under known ecological constraints (van Oevelen et al., 2010). Calculating ensembles of plausible networks accounts for the various configurations of energy flows that may exist in the empirical system, thereby introducing uncertainty of resultant ecosystem indicators. The uncertainty in the ecosystem indicators may provide potentially richer views of ecological system function variability (Hines et al., 2018; Scharler and Borrett, 2021; Waspe et al., 2018).

## 1.2 Aims & Objectives

Currently, neither LIM nor LIM-MCMC are used to their full potential in management. While single network solutions may be easier to calculate and communicate, they ignore variability in the input data, and often take extreme values at the edge of the solution space. These extreme values, although still plausible, may not necessarily be the most representative of the actual ecosystem state (Guesnet et al., 2015; Kones et al., 2006). Ensembles of plausible solutions address the issue of incorporating input data variability, therefore providing more robust estimates of ecosystem function, but are difficult to communicate in a meaningful way to ecosystem managers. Using food web ensembles and select ENA indicators describing ecosystem function in a highly variable case study system, we aimed to 1) explore the differences in ecosystem network properties derived from single solution food webs and ensembles of plausible food webs, and 2) investigate if ensemble methods can provide more robust estimates of ecosystem function than single solution methods.

## 2 Methods

### 2.1 Case study site

Estuaries are highly productive and naturally variable environments given their embedded nature between terrestrial, freshwater, and marine environments (Mahoney and Bishop, 2017). As the interface between these environments, estuaries experience a large variability in conditions that influence ecosystem structure and function, and are therefore vulnerable to compounded effects of global change from each of these environments (Poloczanska et al., 2007). We selected uMdoti Estuary ( $29^{\circ}39'2.1348''\text{S}$ ,  $31^{\circ}7.'44.9328''\text{E}$ ) located on the east coast of South Africa (Figure 1) as our case study site for this investigation. uMdoti Estuary is a perched, large predominantly closed estuary (Van Niekerk et al., 2019b) classified as heavily modified (Skowno et al., 2019; Van Niekerk et al., 2019c), due to very high pressures of pollution (DWA, 2013), siltation (DWA, 2013), and high pressures of flow modification, habitat loss, and invasive fish (Van Niekerk et al., 2019a).

During the study period (2014 – 2016), the region was experiencing an extended drought, limiting freshwater flow into the estuary (Scharler et al., 2020). Freshwater flow was further constricted by the ongoing water abstraction from Hazelmere Dam upstream of the estuary (Brooker and Scharler, 2020). The limited freshwater flow lead to extended mouth closure conditions, with a single mouth breach event between July and August 2015 (Scharler et al., 2020). During a mouth breach event, the estuary opens to the ocean, which allows for system water renewal and flushing (removal of nutrient build up), salinity mixing, and estuarine species recruitment into the estuary (Froneman, 2018; Slinger et al., 2017). For this investigation, the mouth breach event serves as the single acute “system disturbance” during the study period.

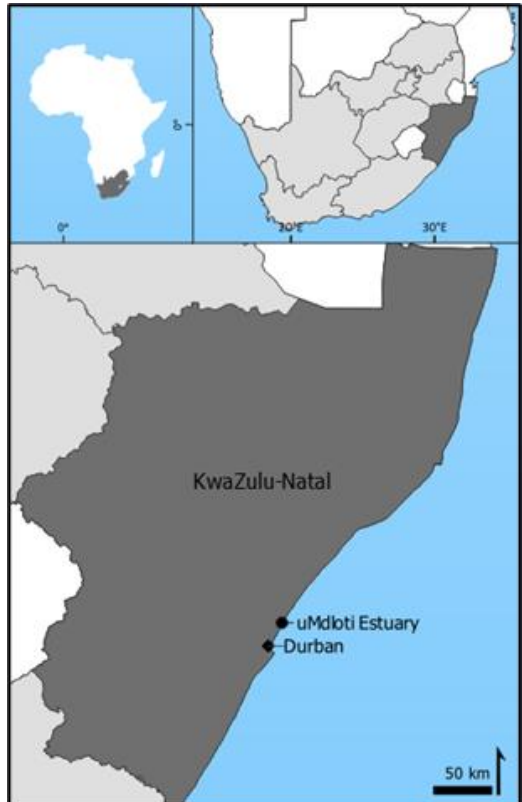


*Figure 1: Location of uMdoti Estuary on the east coast of South Africa and proximity to the nearest city Durban, eThekwin Municipality.*

## 2.2 Data collection & food web model construction

Monthly *in situ* data were collected at three sites (lower, middle, and upper reaches) in uMdloti Estuary during 2014 – 2016. Collected data included physicochemical data, phytoplankton concentration, microphytobenthos concentration, suspended particulate organic matter concentration, sedimented particulate organic matter concentration, and abundances of meiofauna, macrozoobenthos, and zooplankton. Using the *in situ* ecological data, together with empirical data from various published and grey literature, we constructed thirteen monthly food web models to capture temporal ecosystem function before and after the breach event. For technical details on food web model construction we refer the reader to Fath et al., 2007; and Scharler and Borrett, 2021.

Briefly, each monthly food web model topology (structure) was first determined in terms of nodes (species or functional groups) and the trophic links between them. Additional links included egestive flows of material to detrital compartments, and boundary flows of respiration, imports, and exports. We parameterised the food web models by assigning ‘weights’ to each node and inequalities (lower and upper constraints) to each flow in terms of a thermodynamically-conserved model currency (in carbon units  $\text{mgC}\cdot\text{m}^{-2}$  for node biomass,  $\text{mgC}\cdot\text{m}^{-2}\cdot\text{d}^{-1}$  for flow inequalities) (Borrett et al., 2018; van Oevelen et al., 2010). In LIM modelling, it is recommended that inequalities are defined for flows rather than equalities to incorporate ecologically appropriate data variability (Hines et al., 2018; Robson et al., 2018; Scharler and Borrett, 2021; Waspe et al., 2018). We included mass-balance equations for all living compartments  $C = P + R + U$  where input flows of each compartment (consumption (C) or gross primary production (GPP)) is equal to the sum of output flows from the compartment, namely production (P), respiration (R), and unused material/energy (U) (Fath et al 2007). Final model structure in terms of number of living nodes, non-living nodes, externals, internal flows, and boundary flows are summarised in Table 1.

*Table 1: Food web model structure of uMdloti Estuary for the thirteen months included in the time series*

Date	Living Nodes	Non-Living Nodes	Externals	Internal flows	Boundary flows
Apr-15	28	2	33	295	62
May-15	27	2	32	277	60
Jun-15	29	2	34	300	64
Aug-15	24	2	29	245	54
Sep-15	30	2	35	339	66
Oct-15	30	2	35	333	66
Nov-15	28	2	33	293	62
Dec-15	27	2	32	308	60
Jan-16	31	2	36	362	68
Feb-16	29	2	35	307	65
Mar-16	28	2	33	275	62
Apr-16	29	2	34	276	64
Jun-16	24	2	29	216	54

## 2.3 Solving food web network solutions

A popular software method of using LIM to calculate single network solutions and ensembles of plausible networks is with open-source R and R package **LIM (v 1.4.6)** (van Oevelen et al., 2010), and embedded R package **limSolve (v 1.5.1+)** (Soetaert et al., 2009). We first coded parameterised food web models into LIM declaration files using novel translation tools “autoLIM” (Gerber et al., n.d.).

### 2.3.1 Single food web solutions

Using the LIM declaration files with R packages **limSolve** (Soetaert et al., 2009) and **LIM** (van Oevelen et al., 2010), we calculated three single food web solutions for each month using algorithms 1) Least Squares with Equalities and Inequalities (LSEI) (Haskell and Hanson, 1981) with the `lse1()` function, 2) Weighted Least Distance Programming with equality and inequality constraints (LDEI) (Lawson and Hanson, 1995, 1974) with the `ldei()` function, and 3) Central solution (Soetaert et al., 2009) with the `xranges()` function.

### 2.3.2 Ensemble food web solutions

To calculate ensembles of plausible food web networks per month, we used the LIM declaration files and a MCMC “mirror” algorithm via the `xsample()` function in R package **LIM** (Van den Meersche et al., 2009; van Oevelen et al., 2010). The default starting point for the “mirror” algorithm is estimated via LSEI, thereafter the algorithm iteratively samples the solution space based on a user-defined proposal distribution width (jump size) where each returned sample is one plausible food web solution. The mirror algorithm uses the inequalities of the solution space as reflection panes (Van den Meersche et al., 2009) to mirror the MCMC algorithm back into the solution space. Mirroring the MCMC algorithm back into the solution space reduces the possibility of high rejection rates and, therefore, is more efficient for high-dimensional problems such as food webs (Van den Meersche et al., 2009).

In this study, we selected the default starting solution (LSEI) (Van den Meersche et al., 2009), a jump size of  $0.5 \text{ mgC} \cdot \text{m}^{-2} \cdot \text{d}^{-1}$ , and 10,000 iterations. In food web studies, the number of iterations can vary from 1000 (Horn et al., 2017) to 200 million (Kelly et al., 2019), and jump size selection has been based on flow medians (Chaalali et al., 2015), or defaulted to an internally calculated jump size (Van den Meersche et al., 2009). For this study, we selected the jump size and number of iterations based on the need to balance sampling efficiency with computation time. To estimate if the solution space was well-sampled using the selected jump size and number of iterations, we used we used a combination of traceplots and running means plots to assess convergence of the marginal probability function of select flows to the target distribution of the solution space (Roy, 2020; Saint-Béat et al., 2020, 2013).

## 2.4 Ecological Network Analysis

We applied Ecological Network Analysis (ENA) to the single food web solutions and the ensembles of plausible food web solutions using the `get.ns()` function in R package **enaR** (v.3.0.0) (Lau et al., 2017). The `get.ns()` function solves for many different ENA indicators (> 93 indicators), with each indicator describing a different aspect of the system. The inherent complexity of ecosystems and number of ENA indicators has led researchers (and practitioners) to focus on a few macro-scale indicators that consistently give impression of the system function and productivity, allow for comparison across systems or timescales, and can be potentially communicated in a meaningful way to ecosystem managers. In particular, we focus on three ecological indicators that have recently been recommended for policy inclusion (de Jonge and Schückel, 2021; Fath et al., 2019; Safi et al., 2019) (Table 2).

The first, Total System Throughflow ( $TST_{flow}$ ), is an extensive measure of how much energy passes through the system, characterising the overall size and activity of the system (Patten, 1995). More productive systems have a higher  $TST_{flow}$ , which is also indicative of favourable conditions for primary production at the base of all ecosystems. The second indicator, Finn Cycling Index (FCI) (%) (Finn, 1980, 1976), is an intensive measure of the fraction of  $TST_{flow}$  that is cycled and shows how capable the system is at reusing a single unit of flow (Safi et al., 2019) (Table 2). Higher cycling can be interpreted as an indicator of stress (Odum, 1985; Pezy et al., 2018; Scharler and Baird, 2005; Tecchio et al., 2015), but can also describe a system's ability to self-sustain its function despite external perturbations (Saint-Béat et al., 2015). The Detritivory:Herbivory ratio (D:H) characterises the reliance of trophic level II (detritivores and herbivores) on primary producers (plant material) and/or detritus (dead organic matter) to fuel the food web (Latham, 2006; Ulanowicz and Kay, 1991) (Table 2). A high D:H ratio indicates that detritus in that particular system is important for medium cycling such as carbon recycling, and can indicate system maturity (Odum, 1969).

*Table 2: The select system-level ecological network analysis (ENA) indicators used to describe ecosystem function*

Ecological Indicator	Abbreviation	Equation
Total System Throughflow <sup>†</sup> ( $\text{mgC} \cdot \text{m}^{-2} \cdot \text{d}^{-1}$ )	$TST_{flow}$	$TST_{flow} = \sum_{i=1}^n T_i, \text{ where}$ $T_i^{in} = z_i + \sum_{j=1}^n f_{ji}; T_i^{out} = y_i + \sum_{j=1}^n f_{ij}$ $\text{At steady state, } T_i^{in} = T_i^{out} = T_i$
Finn Cycling Index <sup>#</sup> (%)	$FCI$	$FCI = \frac{\sum TST_{ci}}{TST_{flow}} * 100$
Detritivory:Herbivory Ratio <sup>\$</sup>	$DH$	$DH = \frac{\sum \text{Detritivory}}{\sum \text{Herbivory}}$

References: <sup>†</sup>(Ulanowicz, 2004, 1986), <sup>#</sup>(Finn, 1980, 1976), <sup>\$</sup>(Ulanowicz and Kay, 1991)

From the ensemble network solutions, we further calculated nodal throughflow and nodal cycling to determine the contributions of each node to the system-level indicators of  $TST_{flow}$  and FCI. For each plausible food web, we calculated nodal throughflow with the `enaFlow()` function in R package **enaR** (Lau et al., 2017). We developed a custom function `nodeCycle()`, based on `enaFlow()` function, to calculate nodal cycling on one food web solution (Supplemental Information 1). We applied `nodeCycle()` over all plausible solutions using the base R function `lapply()`.

## 2.5 Statistical Analysis

### 2.5.1 Pairwise relationships

We investigated temporal relationships between ecologically related flows and ecological indicators from each solution method through correlation methods, using each month as a sample point. For each of the single network solutions, we used the absolute value for each flow and ecological indicator per month. From the ensembles, we used the median value for each flow and ecological indicator as a representative point of the ensemble. Since we had a small sample size per group ( $n = 13$ ), it was important to determine the distribution of the variables to determine an appropriate statistical test. For each solution type (central, LSEI, LDEI, ensembles), we evaluated the variables of interest for normality using the Shapiro-Wilks test for normality (Supplementary Material 2, Table SI2 1). Where the variables showed evidence of non-normality ( $p > .05$ ), we applied a log-transformation and again evaluated for normality. Based on the normalised values, we applied Pearson correlation analysis to determine relationships between the relevant variables per network solution type. We further compared the correlations between the solution types using Fisher's  $z$  test.

### 2.5.2 Comparison of ensembles

Given the generally large number of samples (iterations), non-independence of samples, and commonly non-normally distributed values (Scharler and Borrett, 2021), parametric statistical analyses are often not appropriate to compare ensemble ecological indicators between time steps (Niquil et al., 2020; Tecchio et al., 2016). Parametric statistical tests will often return statistical significance, even if the actual differences are negligible (Tecchio et al., 2016). In food web modelling, an alternative to parametric statistical tests is Cliff's Delta (Cliff, 1993), which is a non-parametric effect size measure (ESM) that has been successfully used in statistical comparisons of ENA indicators between unique time and spatial steps (Macbeth et al., 2011; Meddeb et al., 2019; Niquil et al., 2020; Tecchio et al., 2016; van der Heijden et al., 2020). For this study we compared select monthly ecological flows and indicator ensembles with Cliff's Delta using the function `cliff.delta()` in R package **effsize** (v3.4.3) (Torchiano, 2020). We considered pairwise comparisons to be significantly different if Cliff's Delta was medium ( $0.33 \geq |\delta| < 0.474$ ) or large ( $|\delta| \geq 0.474$ ) (Table 3).

Table 3: Cliff's Delta values and magnitudes (Cliff, 1993; Macbeth et al., 2011) indicating statistical significance

Cliff's Delta	Magnitude	Indicative of significant differences?
$ \delta  < 0.147$	Negligible	No
$0.147 \geq  \delta  < 0.33$	Small	No
$0.33 \geq  \delta  < 0.474$	Medium	Yes
$ \delta  \geq 0.474$	Large	Yes

## 3 Results

---

### 3.1 Comparing network properties from single & ensemble solutions

#### 3.1.1 Flows

For the select flows presented in this study (in units of  $\text{mgC}\cdot\text{m}^{-2}\cdot\text{d}^{-1}$ ), the flow values calculated from the single solutions LDEI and LDEI generally reflect similar temporal patterns to the ensemble solution distributions, although often at the edges or extreme tails of the ensembles (Figure 2). The flow values calculated from the central solution also generally followed the ensemble trend but were often extreme underestimates or overestimates of the ensemble distributions (Figure 2, Table SI3 1). Single network solution values and ensemble distributions for flows Net Primary Production (NPP) and Total Herbivory tend to follow a seasonal pattern, with lower values in the winter months and higher values during the summer months (Figure 2, Table SI3 1). Total Detritivory calculated from single network solutions were generally low throughout the study time period, with moderate increases in Sep 2015 and during summer months February – March 2016 (Figure 2, Table SI3 1). However, Total Detritivory medians, calculated from ensemble medians, always reflected higher estimates in comparison to the single network solutions (Figure 2, Table SI3 1). Both ensemble and single network solutions indicate generally low Primary Producer Sink (primary producer material to detritus via egestive and mortality flows) throughout the study time period, with the lowest sinks occurring immediately after the system breach in August and September 2015 (Figure 2, Table SI3 1).

#### 3.1.2 Ecological Indicators

For the select ecological indicators presented in this study, the single solutions and ensemble distributions show that uMdoti Estuary ecosystem during the drought period was generally characterised by a reliance on primary producers to fuel the food web, lower cycling, and seasonal summer increases in system activity (Figure 3). Immediately after the system disturbance (mouth breach), the Detritivory:Herbivory ratio (D:H) increased, and thereafter decreased once the mouth closed and remained closed (Figure 3). D:H values from single solutions LSEI and LDEI closely followed the D:H ensemble trend, often in the extreme ends of the distributions, whereas D:H values calculated from the central solution often overestimated the ensemble (May 2015, August 2015, September 2015, November 2015) (Figure 3, Table SI3 2). System cycling, characterised by Finn Cycling Index (FCI) (%) followed a similar trend to D:H, increasing in the months immediately after the system breach, and decreasing once the mouth closed and remained closed. The FCI calculated from the single network solutions often followed the same trends as the ensembles, except in the months immediately after the mouth breach, where single solutions tended to underestimate (August 2015) and overestimate (September 2015) the values from the ensemble distributions (Figure 3, Table SI3 2). System activity, characterised by Total System Throughflow ( $TST_{\text{flow}}$ ) ( $\text{mgC}\cdot\text{m}^{-2}\cdot\text{d}^{-1}$ ) showed seasonal temporal trends in ensemble distributions, increasing in summer months and decreasing in winter months (Figure 3, Table SI3 2). System activity calculated from single network solutions follows a similar seasonal trend as the ensemble distributions but were almost always in the lower tail thereof (Figure 3, Table SI3 2).

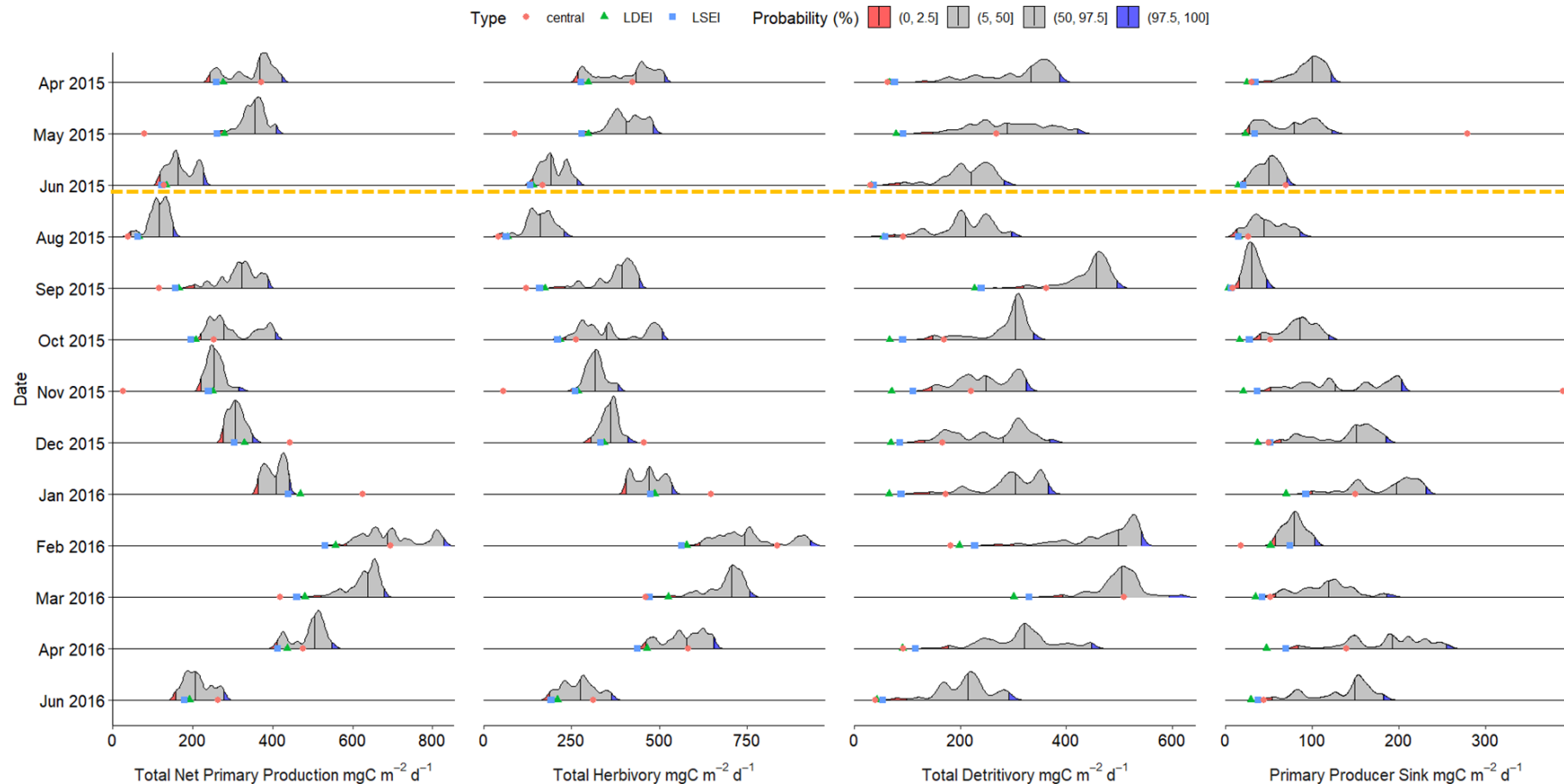


*Figure 2: Density distributions of select flows ( $\text{mgC} \cdot \text{m}^{-2} \cdot \text{d}^{-1}$ ) calculated on 10,000 plausible uMdoti Estuary food web networks per month, with lower (2.5 %) and upper (97.5 %) tails of the distribution highlighted in red and blue, respectively, and grey highlights 95 % confidence intervals of the ensemble means. Ensemble medians are indicated as black lines through the distributions. The same flows calculated from the single network solutions Least Distance with Equalities and Inequalities (LDEI), Least Squares with Equalities and Inequalities (LSEI), and the central solution (central) are plotted together with the ensemble distributions indicating their relative positions within the ensemble distributions. Dashed orange line indicates the system breach.*

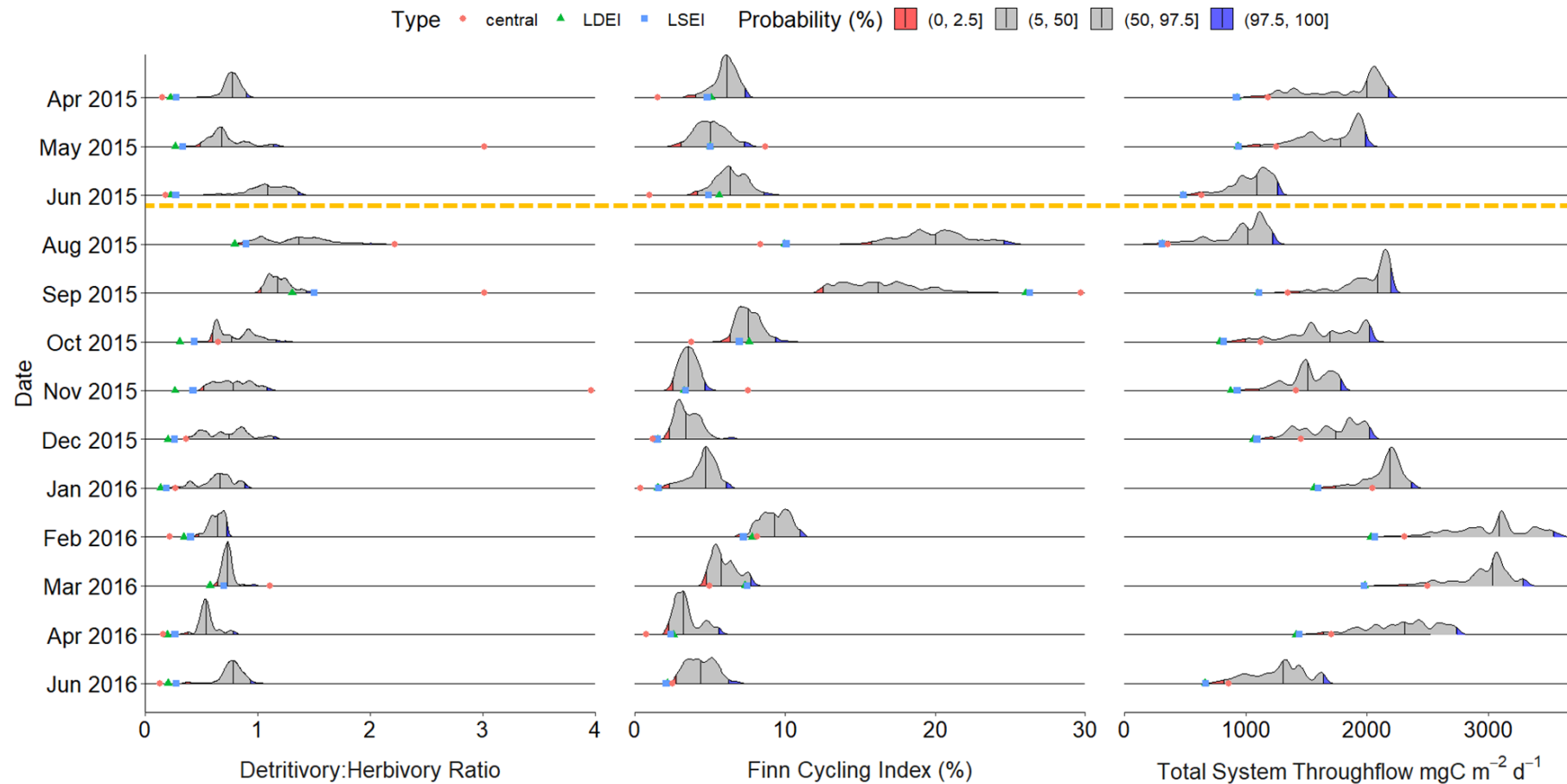


*Figure 3: Density distributions of select Ecological Network Analysis (ENA) indicators calculated on 10,000 plausible uMalloti Estuary food web networks per month, with lower (2.5 %) and upper (97.5 %) tails of the distribution highlighted in red and blue, respectively, and grey highlights 95 % confidence intervals of the ensemble means. Ensemble medians are indicated as black lines through the distributions. The same ecological indicators calculated from the single network solutions Least Distance with Equalities and Inequalities (LDEI), Least Squares with Equalities and Inequalities (LSEI), and the central solution (central) are plotted together with the ensemble distributions indicating their relative positions within the ensemble distributions. Dashed orange line indicates the system breach.*

### 3.2 Frequency of extreme values calculated from single network solutions

For each of the single network solutions (LDEI, LSEI, Central), we calculated the probability of finding a value of any flow or network indicator more extreme than the 95 % confidence intervals (CI) of the means of each ensemble (< 2.5 %, or > 97.5 %). Across all thirteen months, the central solution was less likely to calculate extreme Total Detritivory flow values (38.46 %) than LDEI and LSEI solutions (both 100 %). Further, the central solution was less likely to calculate extreme Primary Producer Sink flow values (61.54 %), than LDEI (92.31 %) and LSEI (76.92 %) solutions (Table 4). However, the central solution was more likely to calculate extreme Total Net Primary Production flow values (53.85 %) than either the LDEI (46.15 %) or the LSEI (38.46 %) solutions. Flow values of Total Herbivory calculated from LDEI solution were less likely extreme values (38.46 %) than those calculated from LSEI (61.54 %) and central (53.65 %) (Table 4).

Finn Cycling Index (FCI) values calculated from the LDEI and LSEI single network solutions were less likely to be extreme values outside of the 95 % confidence intervals of the ensemble means (both 38.46 %) than those calculated from the central solution (84.62 %) (Table 4). Total System Throughflow ( $TST_{flow}$ ) calculated from LDEI and LSEI were always likely to be extreme values (100 %), whereas  $TST_{flow}$  calculated from the central solution were more likely to fall within the 95 % confidence intervals of the ensemble means than not (23.08 %) (Table 4). Detritivory: Herbivory Ratio (D:H) calculated from the LSEI solution were less likely to be extreme values (84.62 %) than those calculated from LDEI and Central solutions (both 92.31 %) (Table 4).

*Table 4: Frequency of flow and ecological indicator values calculated from the single network solutions: Least Distance with Equalities and Inequalities (LDEI), Least Squares with Equalities and Inequalities (LSEI), and the central solution (Central), to fall outside of the 95 % confidence intervals of the ensemble means over thirteen (13) months of analysis in uMdloti Estuary. Select flows ( $mgC \cdot m^{-2} \cdot d^{-1}$ ) include Total Detritivory, Total Herbivory, Primary Producer Sink, and Total Net Primary Production. Select ecological indicators include Detritivory: Herbivory Ratio (D:H), Finn Cycling Index (FCI) (%), and Total System Throughflow ( $TST_{flow}$ ) ( $mgC \cdot m^{-2} \cdot d^{-1}$ ).*

<b>Network Property</b>		<b>LDEI</b>	<b>LDEI</b>	<b>Central</b>
Flows ( $mgC \cdot m^{-2} \cdot d^{-1}$ )	Total Detritivory	100.00	100.00	38.46
	Total Herbivory	38.46	61.54	53.85
	Primary Producer Sink	92.31	76.92	61.54
	Total Net Primary Production	46.15	38.46	53.85
ENA Indicators	D:H	92.31	84.62	92.31
	FCI (%)	38.46	38.46	84.62
	$TST_{flow}$ ( $mgC \cdot m^{-2} \cdot d^{-1}$ )	100.00	100.00	23.08

We further investigated the bias of single solutions to either under- or overestimate flow and ecological indicator values outside the 95 % confidence intervals of the ensemble means. We considered an extreme underestimation to be less than the 2.5 % lower tail of the ensemble distribution, and an extreme overestimation to be above the 97.5 % upper tail of the ensemble distribution. We considered any value within 2.5 – 97.5 % of the ensembles to be equal to, or a likely representation of, the ensemble distribution (Kones et al., 2009).

For the flows combined, we found that flow values calculated from any of the three single solutions were more likely to be underestimates of the ensembles (Figure 4). The flow values calculated from LDEI and LSEI solutions were more likely to be extreme underestimations of the ensembles (67.31 % and 69.23 %, respectively), than those calculated from the central solution (40.38 %) (Figure 4). The central solution was more likely to calculate flows within the 95 % confidence intervals of the ensemble means (48.08 %) than the LDEI and LSEI solutions (both 30.77 %) but was also more likely to overestimate the flow values (11.54 %) than either of the LDEI or LSEI solutions (1.92 % and 0 %, respectively) (Figure 4).

We found a similar trend when we compared the likelihood of calculating extreme ecological indicator values from single solutions, where ecological indicator values calculated from the single solutions were more likely to be underestimates of the ensembles (Figure 4). The ecological indicators calculated from LDEI and LSEI solutions were more likely underestimations of the ensembles (74.36 % and 69.23 %, respectively), than those calculated from the central solution (46.15 %) (Figure 4). While ecological indicator values calculated from the central solution were more likely to be within the 95 % confidence intervals of the ensemble means (33.33 %) than the LDEI and LSEI solutions (23.08 % and 25.64 %, respectively), there was also a greater likelihood that the central solution would result in overestimates of ecological indicators (20.51 %).

When looking at both flows and ecological indicators combined, we found that all three single solutions were most likely to result in underestimations of the ensembles (42.86 – 70.33 %) than to be within the 95 % confidence intervals of the ensemble means, or overestimate the ensembles (Figure 4). However, the central solution was more likely to result in flow and ecological indicator values that fall within the 95 % confidence intervals of the ensemble means (41.76 %) than the LDEI and LSEI solutions, but also was more likely to result in overestimations of the ensembles (15.38 %) (Figure 4).



*Figure 4: Probability (%) of any of the select flows and ecological indicator values calculated with single network solutions Least Distance with Equalities and Inequalities (LDEI), Least Squares with Equalities and Inequalities (LSEI), and the central solution (Central), to be extreme underestimates of the ensembles (< 2.5 %), within the 95 % confidence interval (CI) of ensemble means (2.5 – 97.5 %), or extreme overestimates of the ensembles (> 97.5 %).*

### 3.3 Pairwise relationships between ecologically related flows

In food webs, there are ecologically related relationships between Net Primary Production (NPP), herbivory, and detritivory flows (Heymans et al., 2002). Net Primary Production is an indicator of the primary producer food availability to fuel the food web, either directly via trophic level II taxa consuming more primary producers (herbivory), or indirectly via primary producer die off to the detrital compartment, increasing detrital food resources and an increase in trophic level II feeding on detritus (detritivory) (Fath et al., 2019; Heymans et al., 2002).

We investigated if these ecologically related relationships are consistently reflected in the single and ensemble solutions over the study period, and whether each solution type provides statistically comparable relationships to one another (no significant differences). We found that for all network solution types, there is indeed a strong, positive correlation between primary producer food availability (Total Net Primary Production  $\text{mgC}\cdot\text{m}^{-2}\cdot\text{d}^{-1}$ ) and Total Herbivory ( $\text{mgC}\cdot\text{m}^{-2}\cdot\text{d}^{-1}$ ) in uMdoti Estuary during the study time period (Slope: .99 – 1;  $p < .001$ , two-tailed) (Figure 5A). However this relationship, when derived from the central solution, is statistically significantly different to the relationship derived from the LDEI solution (Fisher's  $z = 2.335$ ,  $p < .05$ , two-tailed), and the relationship derived from the LSEI solution (Fisher's  $z = 2.332$ ,  $p < .05$ , two-tailed) (Table 5). There were no significant differences between correlations derived from the central solution and the ensemble medians ( $p > .05$ , two-tailed), or between the ensemble medians and LDEI and LSEI solutions ( $p > .05$ , two-tailed) (Table 5).

We further compared the relationship between primary producer food availability (Total Net Primary Production  $\text{mgC}\cdot\text{m}^{-2}\cdot\text{d}^{-1}$ ) and Total Detritivory ( $\text{mgC}\cdot\text{m}^{-2}\cdot\text{d}^{-1}$ ) derived from each solution type (Figure 5B). We found a moderate, positive correlation between these variables derived from the LSEI solution (Slope = .61,  $p = .026$ , two-tailed), and a strong, positive relationship when derived from the ensemble medians (Slope = .86,  $p < .001$ , two-tailed) (Figure 5B). We found no significant correlations between these variables when derived from the LDEI solution (Slope = .55,  $p = .051$ , two-tailed), or the central solution (Slope = .08,  $p = .784$ , two-tailed) (Figure 5B). When statistically comparing the correlations derived from each network solution type, we found a significant difference in the correlations derived from the central solution and ensemble medians (Fisher's  $z = -2.683$ ,  $p < .01$ , two-tailed) (Table 5). There were no significant differences between the correlations derived from the central solution to the LDEI and LSEI solutions ( $p > .05$ , two-tailed), or between the correlations derived from the ensemble medians and the LDEI and LSEI solutions ( $p > .05$ , two-tailed) (Table 5).

We compared the relationship between primary producer food availability (Total Net Primary Production  $\text{mgC}\cdot\text{m}^{-2}\cdot\text{d}^{-1}$ ), and how much primary producers contributes to detrital food availability via egestive and mortality sinks (Primary Producer Sink  $\text{mgC}\cdot\text{m}^{-2}\cdot\text{d}^{-1}$ ), derived from each solution type (Figure 5C). We found significant moderate, positive relationships derived from solution type LDEI (Slope = .73  $p = .004$ ) and LSEI (Slope = .79,  $p = .001$ ), but no significant relationships derived from the central solution (Slope = -0.15,  $p = .633$ ) or ensemble medians (Slope = .32,  $p = .288$ ) (Figure 5C). However, when statistically comparing the correlations between network solution types, we found that only the central solution correlation was significantly different to the LDEI solution correlation (Fisher's  $z = 2.424$ ,  $p < .05$ , two-tailed) and the LSEI correlation (Fisher's  $z = 2.744$ ,  $p < .01$ , two-tailed), but not significantly different to the ensemble median correlation ( $p$

> .05, two-tailed) (Table 5). Furthermore, the correlations between LDEI, LSEI, and ensemble medians were not statistically different ( $p > .05$ , two-tailed) (Table 5).

Finally, we compared the relationships between the contribution of primary producers to detrital food availability (Total Primary Producer Sink  $\text{mgC}\cdot\text{m}^{-2}\cdot\text{d}^{-1}$ ) and Total Detritivory ( $\text{mgC}\cdot\text{m}^{-2}\cdot\text{d}^{-1}$ ) (Figure 5D). None of the correlations derived from each solution type showed any significant relationships between these variables ( $p > .05$ , two-tailed), and there were no differences between the correlations derived from each solution type ( $p > .05$ , two-tailed) (Table 5).

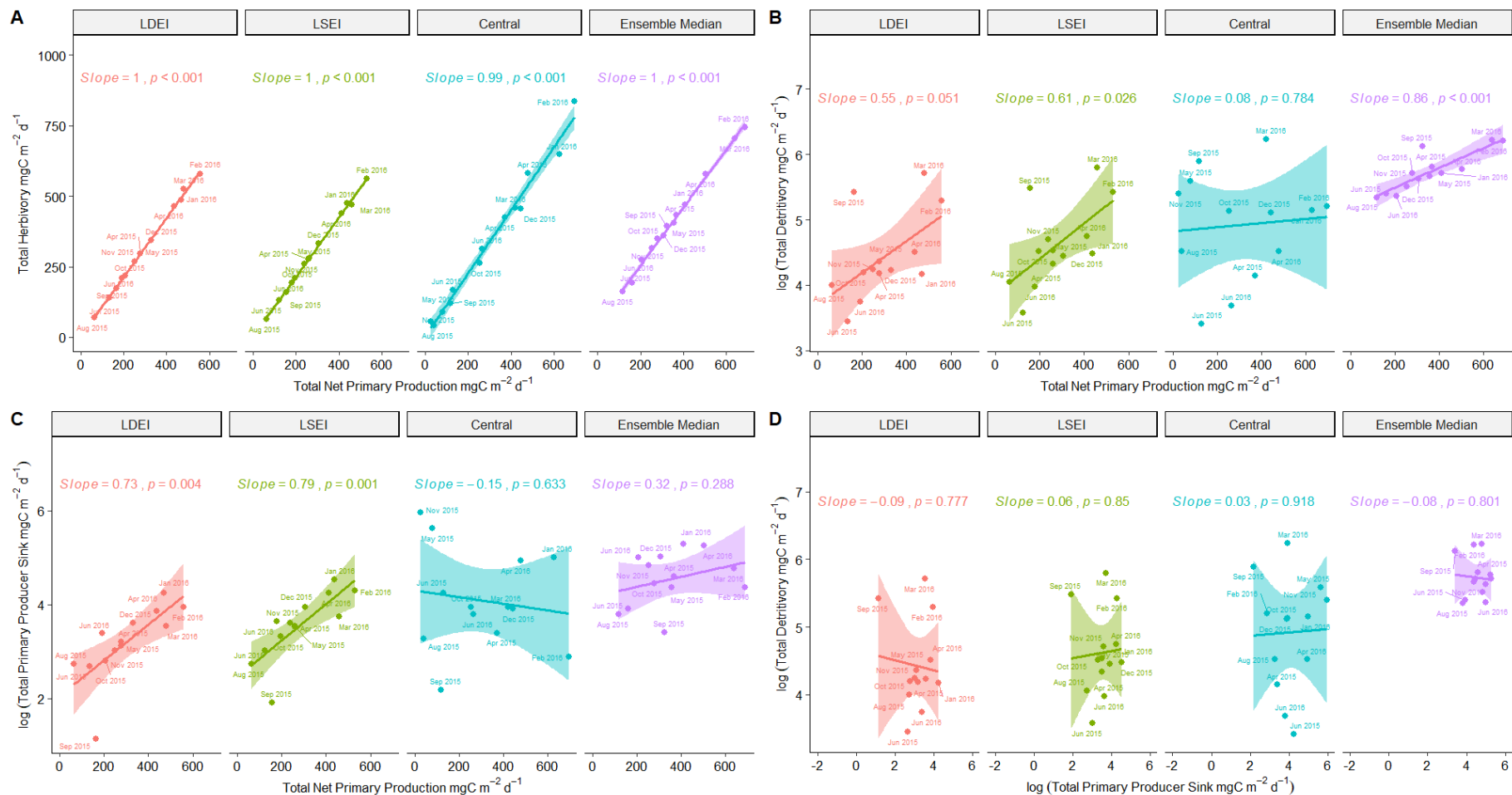


**Figure 5: Pearson Correlations between ecological flows in uMdloti Estuary derived from single solutions (LDEI, LSEI, Central) and ensemble medians ( $n = 13$ ).** A) Total Net Primary Production ( $\text{mgC}\cdot\text{m}^{-2}\cdot\text{d}^{-1}$ ) and Total Herbivory ( $\text{mgC}\cdot\text{m}^{-2}\cdot\text{d}^{-1}$ ), B) Total Net Primary Production ( $\text{mgC}\cdot\text{m}^{-2}\cdot\text{d}^{-1}$ ) and log-scaled Total Detritivory ( $\text{mgC}\cdot\text{m}^{-2}\cdot\text{d}^{-1}$ ), C) Total Net Primary Production ( $\text{mgC}\cdot\text{m}^{-2}\cdot\text{d}^{-1}$ ) and log-scaled Total Primary Producer Sink ( $\text{mgC}\cdot\text{m}^{-2}\cdot\text{d}^{-1}$ ), D) log-scaled Total Primary Producer Sink ( $\text{mgC}\cdot\text{m}^{-2}\cdot\text{d}^{-1}$ ) and log-scaled Total Detritivory ( $\text{mgC}\cdot\text{m}^{-2}\cdot\text{d}^{-1}$ ). Slope indicates the correlation coefficient, p-values indicate the significance of the correlation coefficient (two-tailed, significant if  $p < .05$ ).

*Table 5: Fisher (1925) and Zou (2007) sample estimates ( $r_{1,jk}$ ,  $r_{2,hm}$ ), Fisher's (1925) z-score and p-value, and Zou (2007) 95 % confidence intervals for each correlation between select flows and ecological indicators, between respective network solution methods (LDEI, LSEI, Central, Ensemble Medians). Flows include Total Net Primary Production (NPP), Total Herbivory (Herbivory), Total Detritivory (Detritivory), and Primary Producer Sink (ppSink). Ecological Network Analysis (ENA) indicators include Total System Throughflow ( $TST_{flow}$ ), Detritivory:Herbivory ratio (D:H), and Finn Cycling Index (FCI). Statistical significance is indicated at levels  $p < .05$  (\*),  $p < .01$  (\*\*),  $p < .001$  (\*\*\*)*

Correlations	LDEI / Central						LDEI / Ensemble Median						LDEI / LSEI					
	Estimate		Conf. intervals		Estimate		Conf. intervals		Estimate		Conf. intervals		Estimate		Conf. intervals			
	$r_{1,jk}$	$r_{2,hm}$	$z$	$p$	lower	upper	$r_{1,jk}$	$r_{2,hm}$	$z$	$p$	lower	upper	$r_{1,jk}$	$r_{2,hm}$	$z$	$p$	lower	upper
$\log(D:H) \sim \log(FCI)$	0.886	0.742	0.999	0.318	-0.147	0.570	0.886	0.747	0.976	0.329	-0.150	0.561	0.886	0.886	-0.002	0.998	-0.246	0.245
$\log(D:H) \sim TST_{flow}$	-0.025	-0.084	0.133	0.895	-0.731	0.824	-0.025	-0.579	1.420	0.155	-0.211	1.177	0.886	0.886	-0.002	0.998	-0.246	0.245
$\log(FCI) \sim TST_{flow}$	-0.050	-0.076	0.057	0.954	-0.757	0.798	-0.050	-0.072	0.049	0.961	-0.760	0.795	-0.025	-0.048	0.052	0.959	-0.760	0.797
$\log(ppSink) \sim \log(Detritivory)$	-0.087	0.032	-0.266	0.790	-0.870	0.683	-0.087	-0.078	-0.022	0.983	-0.784	0.769	-0.050	-0.053	0.007	0.994	-0.776	0.781
NPP ~ Herbivory	0.999	0.992	2.335	< .05*	0.001	0.027	0.999	0.998	0.871	0.384	-0.002	0.007	-0.087	0.058	-0.326	0.744	-0.891	0.662
NPP ~ log(Detritivory)	0.550	0.084	1.194	0.233	-0.294	1.111	0.550	0.858	-1.489	0.136	-0.868	0.096	0.550	0.613	-0.211	0.833	-0.671	0.535
NPP ~ log(ppSink)	0.734	-0.146	2.424	< .05*	0.155	1.411	0.734	0.319	1.356	0.175	-0.185	1.042	0.734	0.793	-0.320	0.749	-0.509	0.346
<hr/>																		
LSEI / Central						LSEI / Ensemble Median						Central / Ensemble Median						
Correlations	Estimate		Conf. intervals		Estimate		Conf. intervals		Estimate		Conf. intervals		Estimate		Conf. intervals			
	$r_{1,jk}$	$r_{2,hm}$	$z$	$p$	lower	upper	$r_{1,jk}$	$r_{2,hm}$	$z$	$p$	lower	upper	$r_{1,jk}$	$r_{2,hm}$	$z$	$p$	lower	upper
	0.886	0.742	1.001	0.317	-0.147	0.571	0.886	0.747	0.978	0.328	-0.150	0.561	0.742	0.747	-0.023	0.981	-0.458	0.446
$\log(D:H) \sim \log(FCI)$	-0.048	-0.084	0.081	0.936	-0.749	0.805	-0.048	-0.579	1.368	0.171	-0.229	1.160	-0.084	-0.579	1.288	0.198	-0.256	1.132
$\log(FCI) \sim TST_{flow}$	-0.053	-0.076	0.050	0.960	-0.760	0.795	-0.053	-0.072	0.042	0.967	-0.763	0.792	-0.076	-0.072	-0.009	0.993	-0.780	0.774
$\log(ppSink) \sim \log(Detritivory)$	0.058	0.032	0.060	0.952	-0.757	0.799	0.058	-0.078	0.305	0.760	-0.670	0.884	0.032	-0.078	0.245	0.807	-0.691	0.863
NPP ~ Herbivory	0.999	0.992	2.332	< .05*	0.001	0.027	0.999	0.998	0.868	0.385	-0.002	0.007	0.992	0.998	-1.464	0.143	-0.026	0.002
NPP ~ log(Detritivory)	0.613	0.084	1.405	0.160	-0.209	1.157	0.613	0.858	-1.278	0.201	-0.774	0.132	0.084	0.858	-2.683	< .01**	-1.355	-0.182
NPP ~ log(ppSink)	0.793	-0.146	2.744	< .01**	0.250	1.458	0.793	0.319	1.676	0.094	-0.082	1.091	-0.146	0.319	-1.068	0.285	-1.118	0.374

### 3.4 Pairwise relationships between ecologically related indicators

We compared pairwise relationships (correlations) of ecological indicators, understood as ecologically related, derived from each solution type to establish each solution type's representation of ranges of ecological input data. Ecological indicators Detritivory:Herbivory Ratio (D:H) and Finn Cycling Index (FCI) are understood to be related as an increase in detritivory (and resultant increase in D:H) has been shown to increase the overall cycling (characterised by FCI) of a system (Odum, 1969) (Figure 6A). In our study, we found statistically significant positive linear relationships between D:H and FCI in all single solution and ensemble solution networks (Slope: 0.74 – 0.89,  $p < .05$ , two-tailed) (Figure 6B), in agreement with the expected linear trend. The relationships derived from LDEI and LSEI solutions were identical (Slope = .89,  $p < .001$ , two-tailed) (Figure 6B). The relationship derived from the central solution (Slope = .74,  $p = .004$ , two-tailed) and the ensemble medians (Slope = .75,  $p = .003$ , two-tailed) were similar, with the central solution showing a greater variance and range than the ensemble median (Figure 6B). However, none of the correlations between solutions methods were statistically different from one another ( $p > .05$ , two-tailed) (Table 5).

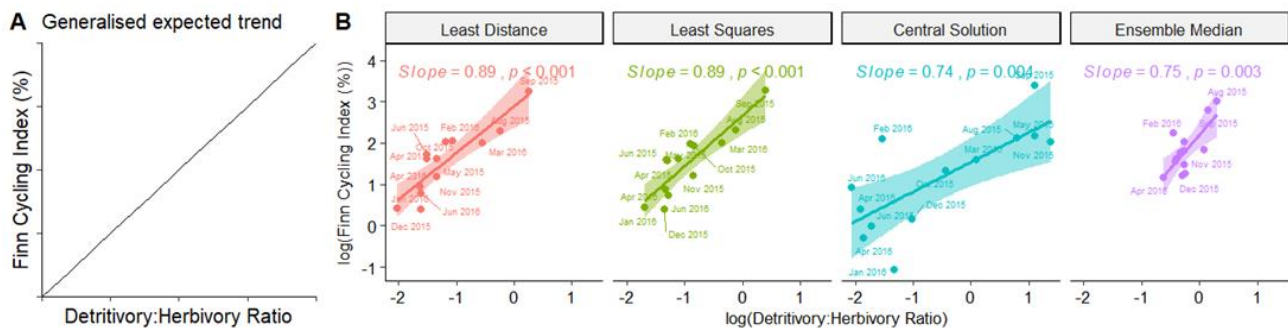


Figure 6: A) Generalized linear relationship between ecological indicators Detritivory:Herbivory ratio (D:H) and Finn Cycling Index (FCI), B) Pearson correlations between Ecological Network Analysis (ENA) indicators D:H and FCI in uMdloti Estuary derived from single network solutions (LDEI, LSEI, Central) and ensemble medians. Slope indicates the correlation coefficient, p-values indicate the significance of the correlation coefficient (two-tailed, significant if  $p < .05$ ). ( $n = 13$ ).

We summarise the rest of the ecological indicator pairwise comparisons in Supplementary Material 4 (Figure SI4 1) as correlations between the ecological indicators (D:H vs FCI, FCI vs TST<sub>flow</sub>) derived from each solution type were not significant ( $p > .05$ , two-tailed), nor were these correlations statistically different between solution types ( $p > .05$ , two-tailed) (Table 5).

## 3.5 uMdoti Estuary temporal ecosystem function

While the focus of this study is to determine methodology differences between single network solutions and ensemble solutions, ecological indicators are only useful if they can be meaningfully compared across spatial and temporal scales (Kones et al., 2009). As single network solutions do not allow for statistical comparisons, we have used the LIM-MCMC derived ecological indicators for the temporal comparison of uMdoti ecosystem function during drought conditions.

### 3.5.1 System-level function

Under drought conditions experienced during the study period, the uMdoti estuary ecosystem showed a consistently low ensemble median Detritivory:Herbivory ratio ( $D:H < 1.08$ ) except for the months August 2015 (1.36) and September 2015 (1.17) immediately after the mouth breach (Figure 7). As an ensemble,  $D:H$  was significantly greater in August and September 2015 as compared to the other months (Cliff's  $|\delta| > 0.474$ , Figure 9). Ensemble distributions also showed an increased variance of  $D:H$  in August 2015 immediately after the breach (Figure 7). The increase in  $D:H$  during August 2015 may be explained by the decline in primary producer food availability, characterised by Total Net Primary Production ( $\text{mgC}\cdot\text{m}^{-2}\cdot\text{d}^{-1}$ ), and subsequent decline in total herbivory flows ( $\text{mgC}\cdot\text{m}^{-2}\cdot\text{d}^{-1}$ ) (Figure 8).

System cycling, characterised by Finn Cycling Index (FCI), was consistently low for all months ( $< 10 \%$ ), except for the months immediately after the system breach (August 2015: 20.02 %, September 2015: 16.17 %) where cycling was much greater (Cliff's  $|\delta| > 0.474$ , Figure 9). Ensemble distributions of FCI during closed mouth conditions immediately after the mouth breach in August and September 2015 show an increased variance as compared to months before the system breach, and months after September 2015 as the mouth state closed and remained closed (Figure 9).

System activity, characterised by Total System Throughflow ( $TST_{\text{flow}}$ ,  $\text{mgC}\cdot\text{m}^{-2}\cdot\text{d}^{-1}$ ), followed a seasonal trend, with higher metabolic activity during the warmer summer months (Figure 7). The seasonal system activity may be explained by the Total Net Primary Production ( $\text{mgC}\cdot\text{m}^{-2}\cdot\text{d}^{-1}$ ), where primary producers are more productive during summer months with longer daylight hours (Figure 8). There was no statistically significant change in system activity immediately after the breach (June 2015 and August 2015, Cliff's  $|\delta| = 0.2$ , Figure 9).

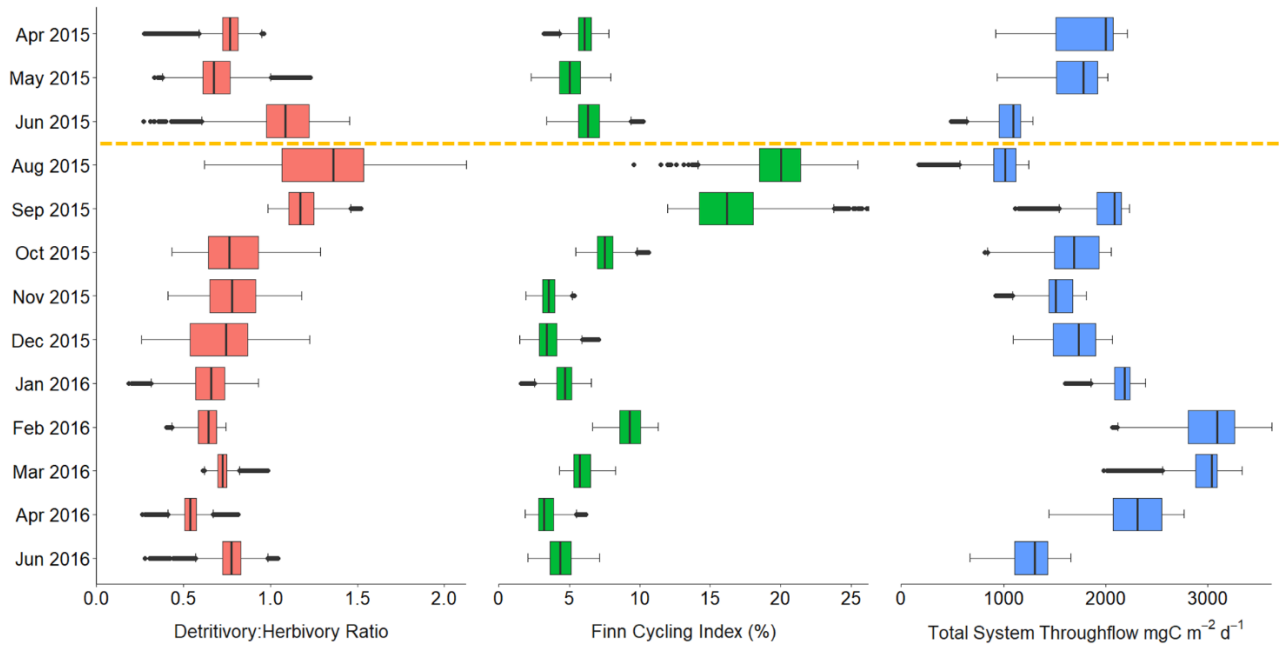


**Figure 7: Temporal variation of uMdloti Estuary ecosystem function characterised by Ecological Network Analysis (ENA) indicators** Detritivory: Herbivory Ratio (D:H), Finn Cycling Index (FCI), and Total System Throughflow (TST<sub>flow</sub>). Lower and upper box boundaries represent 25<sup>th</sup> and 75<sup>th</sup> percentiles, respectively. Lower and upper error lines represent  $\pm 1.5 * \text{IQR}$  (Interquartile Range). Line inside the box represents the median. Filled circles indicate outliers outside of. Dashed orange line indicates the system breach. ( $n = 10,000$ ).

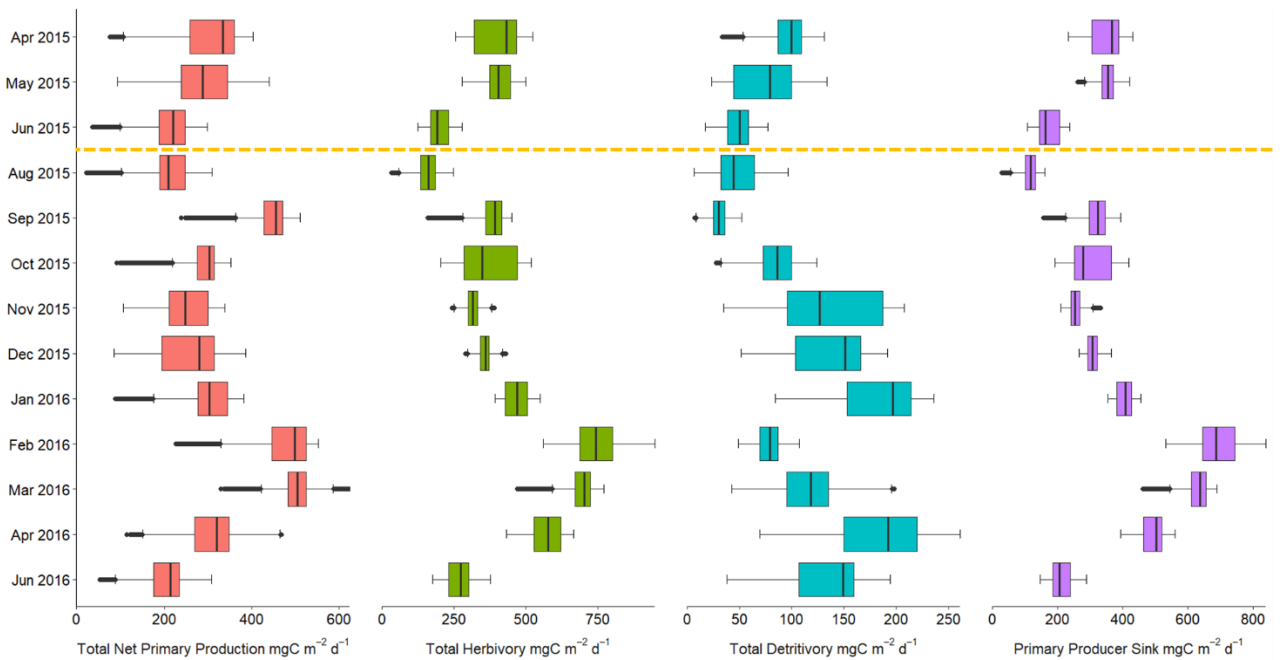


**Figure 8: Temporal variation of select monthly food web flows ( $\text{mgC} \cdot \text{m}^{-2} \cdot \text{d}^{-1}$ ) in uMdloti Estuary.** Lower and upper box boundaries represent 25<sup>th</sup> and 75<sup>th</sup> percentiles, respectively. Lower and upper error lines represent  $\pm 1.5 * \text{IQR}$  (Interquartile Range). Line inside the box represents the median. Filled circles indicate outliers outside of. Dashed orange line indicates the system breach. ( $n = 10,000$ ).

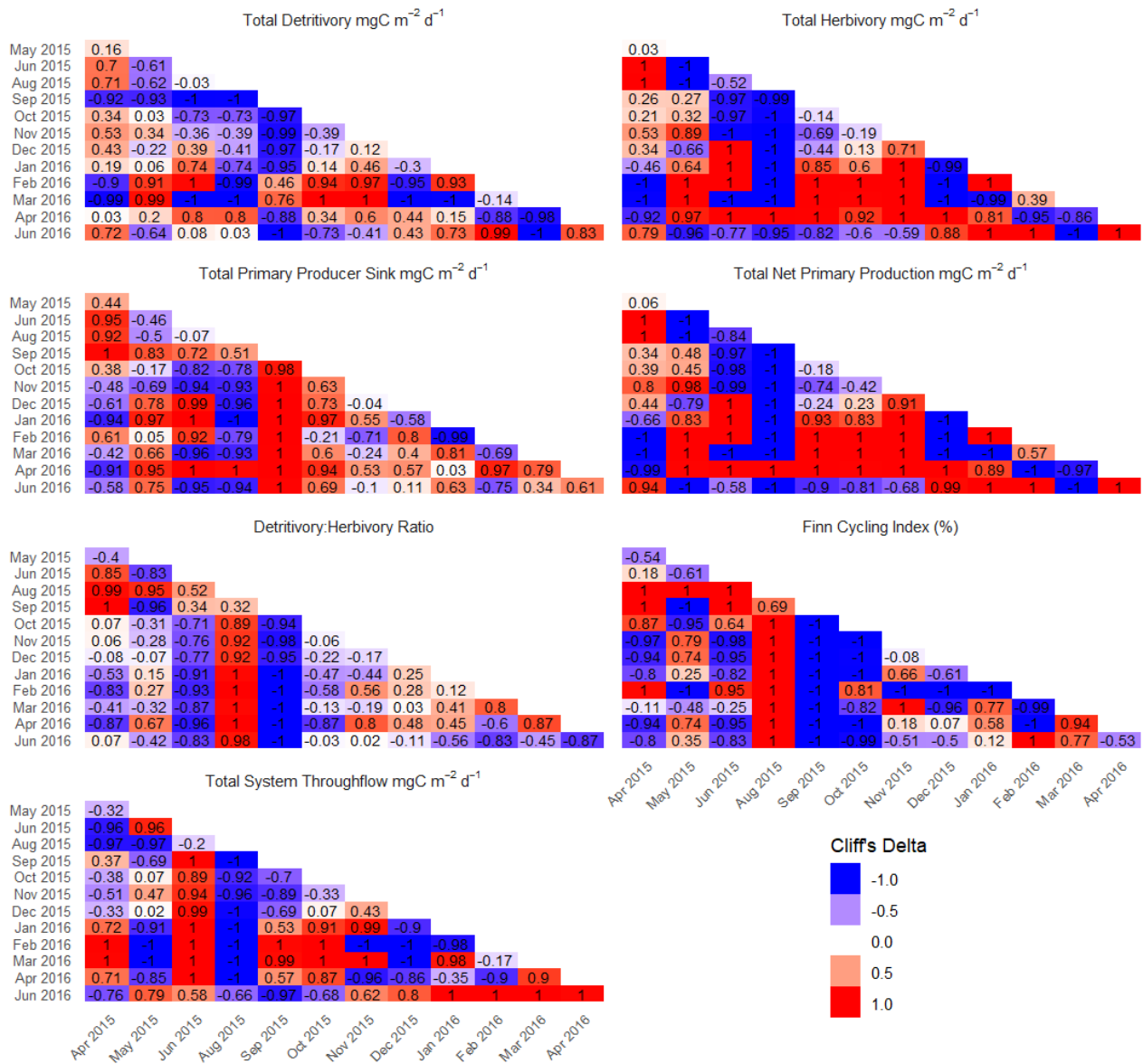


**Figure 9: Variation in monthly ecosystem functioning of uMdloti estuary, characterised by flows ( $\text{mgC m}^{-2} \cdot \text{d}^{-1}$ ) Total Detritivory, Total Herbivory, Primary Producer Sink, and Total Net Primary Production, and Ecological Network Analysis (ENA) indicators Finn Cycling Index (FCI), Detritivory:Herbivory Ratio (D:H), and Total System Throughflow ( $TST_{\text{flow}}$ ). Pairwise Cliff's Delta  $\delta$  magnitudes compared between months (x axis indicates Group 1, y axis indicates Group 2) indicate the degree of variation between months. Red indicates a strong increase, blue indicates strong decrease, white indicate no variation ( $n = 10,000$ ). Absolute values of Cliff's  $\delta$  are considered significant if  $\geq 0.33$ .**

### 3.5.2 Node-level function

Under drought conditions, uMdloti Estuary ecosystem activity was driven by nodal activity of detrital compartments suspended particulate organic carbon (susPOC) and sedimented particulate organic carbon (sedPOC), as well as primary producing microalgae (Phytoplankton and Microphytobenthos), and Oligochaeta (Figure 10). Immediately after the system breach, there was a decline in the nodal activity contributions from freshwater taxa *Corbicula fluminalis* (O. F. Müller, 1774), *Bulinus sp.* (O. F. Müller, 1781), and Chironomidae, but an increase in nodal activity contributions from estuarine taxa, most notably polychaeta Sabellidae, calanoid copepod *Pseudodiaptomus hessei* (Mrázek, 1894) and bivalve *Brachidontes virgiliae* (Barnard, 1984) (Figure 10). After the system breach and prolonged mouth closure, the system activity was more dominated by freshwater taxa than estuarine taxa, except for *B. virgiliae* which persisted activity within the system despite freshwater conditions (Figure 10).

During months before the system breach, system cycling was driven by the nodal cycling of Oligochaeta, Rotifera, and freshwater Chironomidae (Figure 11). In August 2015 immediately after the breach, there were increased contributions to total cycling from estuarine zooplankton, specifically from *P. hessei*, *B. virgiliae*, and freshwater/estuarine Diplostraca (Figure 11). At the same time, contributions to system cycling from Chironomidae, Oligochaeta, and Rotifera rapidly declined. After the mouth closed and remained closed, system cycling once again was attributed to the nodal cycling of freshwater taxa rather than estuarine taxa (Figure 11).

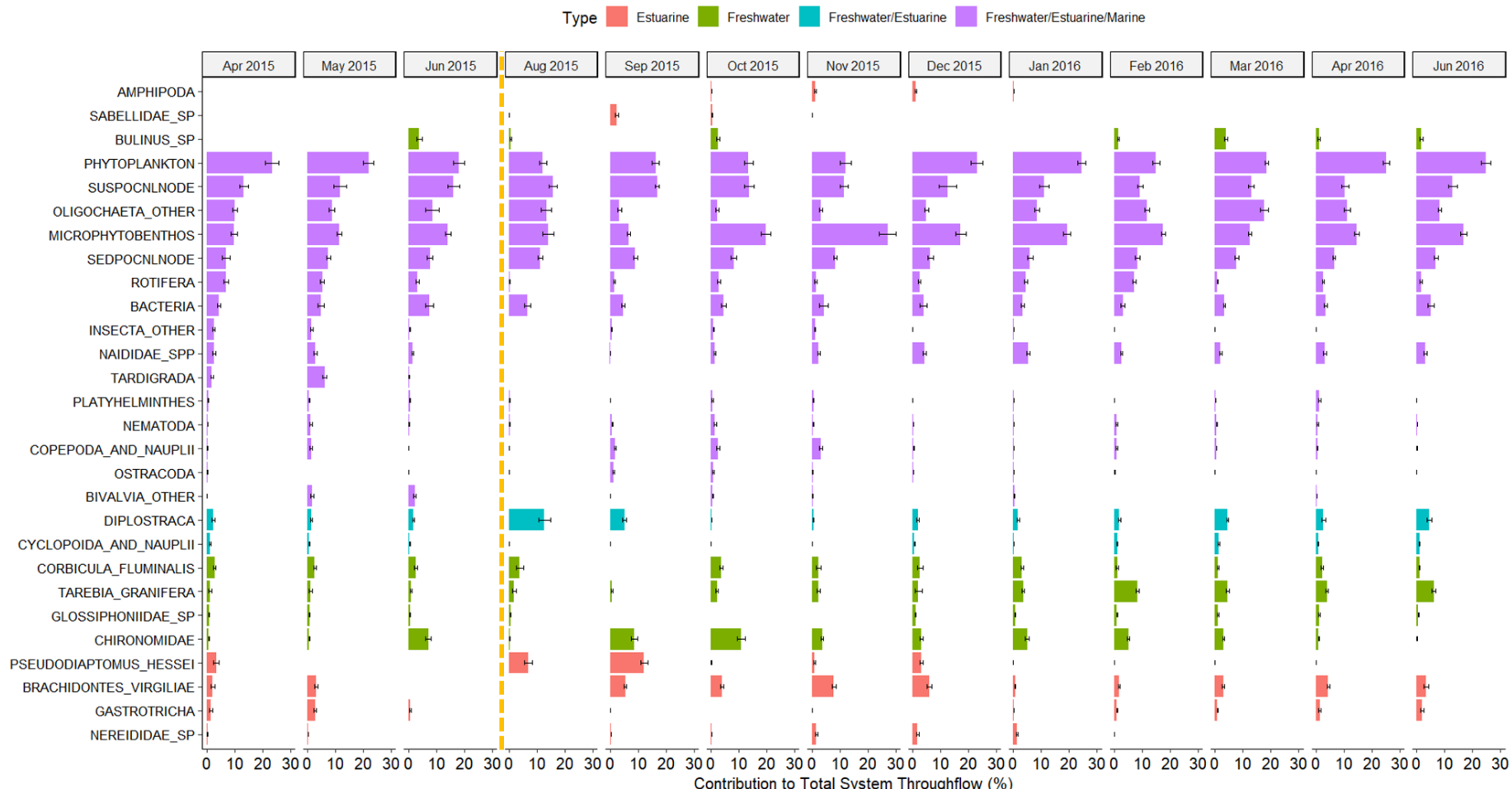


Figure 10: Mean nodal throughflow contribution (%) to Total System Throughflow ( $\text{mgC}\cdot\text{m}^{-2}\cdot\text{d}^{-1}$ ) in uMdloti Estuary ecosystem over thirteen (13) months ( $n = 10,000$ ). Error bars indicate  $\pm 1 \text{ SD}$ . Orange dashed line indicates system disturbance (mouth breach).

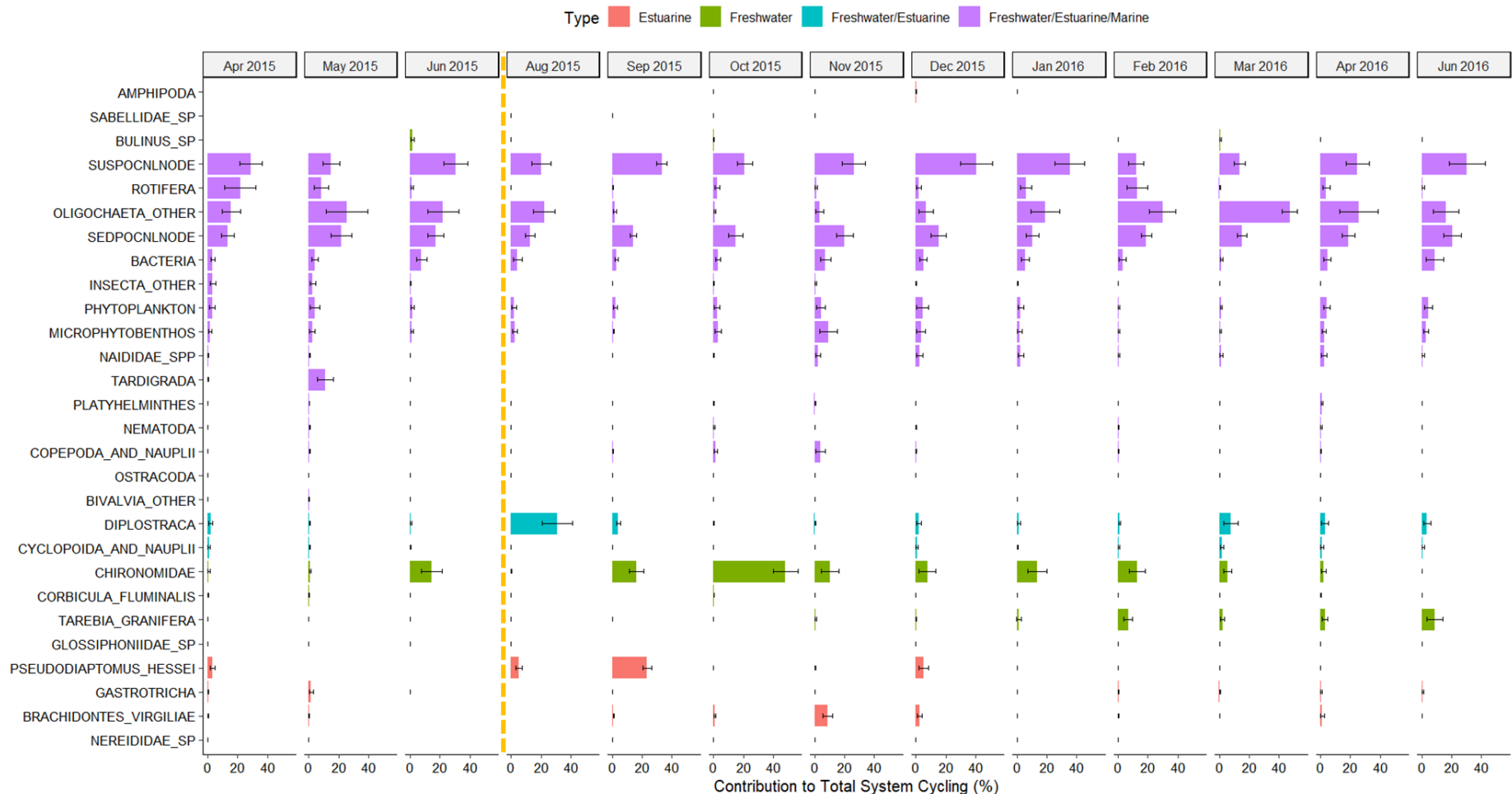


Figure 11: Mean nodal contributions (%) to Total System Cycling ( $\text{mgC} \cdot \text{m}^{-2} \cdot \text{d}^{-1}$ ) in uMloti Estuary ecosystem over thirteen (13) months ( $n = 10,000$ ). Error bars indicate  $\pm 1 \text{ SD}$ . Orange dashed line indicates system disturbance (mouth breach).

## 4 Discussion

---

### 4.1 Can ensemble solutions provide more robust estimates of ecosystem function than single solutions?

#### 4.1.1 Ecological indicators derived from single network solutions

In Linear Inverse Modelling (LIM) problems, the single network solutions Least Distance with Equalities and Inequalities (LDEI) and Least Squares with Equalities and Inequalities (LSEI) are used to solve the simplest (parsimonious) solution (Soetaert et al., 2009; van Oevelen et al., 2010). LSEI is used to calculate a single solution for overdetermined LIM problems (number of independent equations > number of unknowns), whereas LDEI is used to calculate a single solution for underdetermined LIM problems (number of independent equations < number of unknowns) (Soetaert et al., 2009; van Oevelen et al., 2010). Theoretically, if a system is underdetermined (as is often the case in food web LIM problems), LSEI and LDEI should return the same value (van Oevelen et al., 2010). In this study, we found evidence that for most months, the network solutions solved with LSEI and LDEI, and analysed with ENA, returned very similar ecological indicator values, but not identical (Figure 2, Figure 3).

The slight differences in the ecological indicator values could be because of the calculation of the ecological indicators from the network solutions, and not necessarily of the network solutions themselves. From the comparisons of extreme flow value estimates from single solutions (Table 4), it is immediately obvious that in this study, the LDEI and LSEI solutions return different flow values (otherwise they would be equally likely to return extreme flow estimates). Therefore, we can infer that in this study, the LDEI and LSEI solutions did not produce identical network solutions, which is in contrast with van Oevelen et al., 2010. Further work is then required on 1) the causes of the differences between LDEI and LSEI network solutions, and 2) how these differences may or may not propagate themselves in the calculation of ecological indicators.

In this study, flow and ecological indicator values calculated from single solution networks (LSEI, LDEI, Central) are often outside of the 95 % confidence intervals of the ensemble means (Figure 4), indicating that these solutions reflect extreme values that are not representative of the ensembles. We determined that generally, ecological indicators calculated from single network solutions tend to be underestimations of the ensembles (Figure 4). The underestimation in LSEI and LDEI solutions may lie in the algorithm tendency to solve network solutions from a corner of the Euclidean solution space, at the intersection of the inequality constraints (Van den Meersche et al., 2009). These extreme values at the edge of the solution space may not be fair representations of the empirical food web energy flows (Diffendorfer et al., 2001; Kones et al., 2006; Niquil et al., 1998). In agreement with our study, previous studies comparing parsimonious estuarine food web solutions to LIM-MCMC derived ensemble distributions have found that the parsimonious solution is often significantly smaller than the mean ensemble solutions (Kones et al., 2009). In contrast to the similar ecological indicator values derived from parsimonious LSEI and LDEI solutions, the flow and ecological indicator values derived from the central solutions are often largely different from LSEI and LDEI solutions (Figure 2, Figure 3). As the central solution is calculated from the means of the input inequalities (Soetaert et al., 2009), we can infer that the central solution may sample a more *central*, or ecologically representable region of the solution space as

compared to the LSEI and LDEI solutions from the edges of the solution space. However, the central solution is also more likely to overestimate ensemble values than the LDEI or LSEI solutions (Figure 4). We therefore recommend exercising caution when using the central solution as a single network solution, as it is still not representative of the ensembles.

Regardless of whether a single solution under- or overestimates ensemble flow and ecological indicator values, ecological interpretations based on extreme values may not be representative of the empirical system. In an ecosystem management context, management decisions based on extreme outliers describing ecosystem function would not consider the uncertainty of the actual system function, potentially having no effect or the opposite effect of the management intention.

#### 4.1.2 Ecological indicators derived from ensemble network solutions

In this study, the ensembles showed more realistic and robust estimates of ecosystem function within ecological constraints, as compared to the extreme estimates often returned by single network solutions (Figure 3, Figure 4). Ensemble methods preserve the inherent variability of the ecological data, and therefore introduce uncertainty in the model outputs describing ecosystem function that may be more representative of the empirical system (Hines et al., 2018; Waspe et al., 2018). From an ecosystem management perspective, the ensembles provide more information in terms of range of potential ecosystem function, therefore decision makers may find it more comfortable (or appropriate) to make decisions based on this information, rather than the limited information provided by single network solutions, which themselves often describe extreme ecological states.

In addition, the variance within ensembles can be used to detect important shifts in system behaviour due to external perturbations (Tecchio et al., 2016; Tomczak et al., 2013). In this study, Finn Cycling Index (FCI) ensemble variance increased in August 2015 and September 2015 immediately after a system disturbance (mouth breach) (Figure 3). The shift in system function was not detected for August 2015 by any of the three single network solutions (LSEI, LDEI, central), and in September 2015 all the single network solutions overestimated the ensemble FCI (Figure 3). As ecosystem management policy often deals with disturbance events, the ensemble solutions that can detect these disturbances has potential relevance for decision makers. Ensembles of food web solutions further allow for robust statistical comparison of ecosystems across time and space (Figure 9), whereas comparisons between single network solutions are often limited to descriptive studies (Guesnet et al., 2015).

## 4.2 Temporal comparison of uMdloti ecosystem function

Under drought conditions experienced during the study, the generally low Detritivory:Herbivory Ratio (D:H) exhibited by uMdloti Estuary (Figure 7) ecosystem indicates that the system is primarily reliant on primary producers (microalgae) to fuel the food web (de Jonge and Schückel, 2019). The reliance on primary producers indicates that the systems may be less resilient to disturbances affecting the primary producers. The increased D:H immediately after the breach indicates a system shift towards detritivory, perhaps as a response to a lack of primary producers that had been flushed out during the breach. Previous research has shown that an increase in D:H may result from disturbances to the system (de Jonge and Schückel, 2019; Niquil et al., 2014; Schückel et al., 2015). Previous work has also found positive relationships between D:H and primary producer food resource availability (Chrystal and Scharler, 2014). Alternatively, an increase in primary producer food resources could contribute to the detrital pool via sinks due to die off. The increase in detrital food resources could lead to an increase in detritivory, leading to an overall increased D:H ratio (Heymans et al., 2002). In uMdloti, the increase in D:H after the breach may be because of the decreased primary producer food availability, hence the systems shift towards detritivory (Figure 8).

The generally low temporal cycling of uMdloti Estuary is indicative of a system that is dependent on external inputs of material/energy to maintain function (de Jonge et al., 2019). uMdloti Estuary and its river courses receive treated waste effluent from three wastewater treatment works (WWTW) which supplies a constant trickle of nutrients into the system (Brooker and Scharler, 2020). The increase in system cycling immediately after the system disturbance (breach event) is in agreement with previous literature suggesting that a change in FCI can indicate a system disturbance (Tecchio et al., 2016). However, cycling is also an indicator of how well the system can rely on itself to maintain function despite external disturbances (Saint-Béat et al., 2015). Given the persistently low cycling of this system, we suggest that uMdloti Estuary ecosystem is generally less resilient to external perturbations, as it relies on boundary inputs to maintain its function (Figure 7).

Seasonal trends of uMdloti Estuary system activity can be related to natural temperature variability, which may lead to a change in ecosystem function (de la Vega et al., 2018). Previous research of the Brouage mudflat, France, showed that system activity was greater during warmer months due to increased metabolic activity (Leguerrier et al., 2007). Changes in ecosystem function can be related to natural or anthropogenically-induced perturbations in physical, chemical, and biological perturbations (Le Guen et al., 2019), therefore, we cannot make the assumption that changes in system activity are only related to temperature. To better understand the effects of external perturbations on system activity, future research could include investigating the quantitative relationships between seasonal physical drivers, such as temperature, to better elucidate the causes of changes in system activity.

Ecosystem level indicators are often calculated as aggregated values of nodal activity. We can therefore interrogate the node level ecological indicators to explain the variances displayed in the ecosystem level ecological indicators. Interrogating the node level indicators allows us to go "back to the field" to tie overall system function with the underlying biology of the system components. By investigating nodal throughflow, we found that uMdloti Estuary system activity is dominated by detrital and primary producing nodes (Figure 10). This finding is in agreement with previous research suggesting that system activity in food web systems is often concentrated in the detrital and primary producing nodes (Borrett, 2013).

Through investigating individual nodal contributions to system cycling, we found that the increased system cycling immediately after the mouth breach was due to increased cycling activity by estuarine taxa (Figure 11). The breach event led to recruitment of estuarine taxa into the estuary, in turn, the increased estuarine taxa diversity within the estuary. The high nodal cycling exhibited by the estuarine taxa contributed to an overall increase in system level cycling immediately after the breach. This highlights the importance of estuarine species diversity in maintaining system cycling. A system with higher cycling provides a potential buffer against system changes due to external disturbances such as wastewater pollution and climate change. From an ecosystem management perspective, it may be desirable to manage ecosystems in a way that increases system cycling, thereby increasing the system's ability to self-sustain its function despite global change-induced perturbations (Saint-Béat et al., 2015). In our study, we showed that system cycling increases with an increase in estuarine taxa diversity immediately after the mouth breach. Natural mouth breach frequency is an important factor in maintaining ecosystem function (Froneman, 2018). The mouth breach frequency is dependent on rainfall and degree of freshwater abstraction from the estuary and river components. While managers cannot control exogenous disturbances such as drought, managers can manage the level of water abstraction from the system to increase the frequency of natural mouth breaching events.

## 4.3 Limitations of ensemble methods in ecological modelling

### 4.3.1 LIM-MCMC algorithm parameter selection

The range of sampled food web solutions is dependent on how well the Euclidean space is sampled via the LIM-MCMC algorithm. LIM-MCMC algorithms sample the solution space (within ecologically relevant constraints) based on algorithm parameters, namely the initial (starting) point, the proposal width (jump size), and iterations (number of solutions). If the solution space is well-sampled, the solutions will return a range of multiple plausible solutions that are more representative of the input data variability, reflecting a greater range of potential flow configurations. In contrast, a poorly sampled solution space results in multiple plausible food web solutions that are not representative of the input data variability (Figure 12). High dimensional datasets, such as food webs, often require larger jump sizes and iterations to solve an adequate number of ecologically representative solutions (Nemeth and Fearnhead, 2021; Waspe et al., 2018). However, the selection of algorithm starting point, jump size, and iterations to sample adequately the solution space is case-study dependent, therefore there are no set recommendations (van Oevelen et al., 2010; Waspe et al., 2018). Regardless of the food web model, the selection of the LIM-MCMC parameters should not be arbitrary, but rather be selected as to adequately sample the solution space within a reasonable computation time.

In this study, we selected the default starting solution (LSEI) (Van den Meersche et al., 2009) for the LIM-MCMC algorithm. The initial LSEI solution often returns solutions from the corner of the solution space, which may result in food web solutions that reflect more extreme, and less likely ecological estimates. Therefore, the LSEI solution we used as a starting point may not necessarily be the most efficient, nor the most appropriate starting point algorithm. Instead, we can find alternative starting points that are more appropriate for ecological LIM problems. In our study, we found that the central solution was less likely to result in extreme ecological indicator values than the LSEI or LDEI solutions (Figure 4). The central solution is calculated from the means of the input data constraints (Soetaert et al., 2009) and may allow the LIM-MCMC algorithm to begin sampling the solution space in a more central region, rather than near the edges of the solution space (Van den Meersche et al., 2009; van Oevelen et al., 2010). In future studies, the central solution may offer a better starting point for the LIM-MCMC sampling algorithm, possibly returning less extreme, and more ecologically representative solutions given the ecological input constraints.

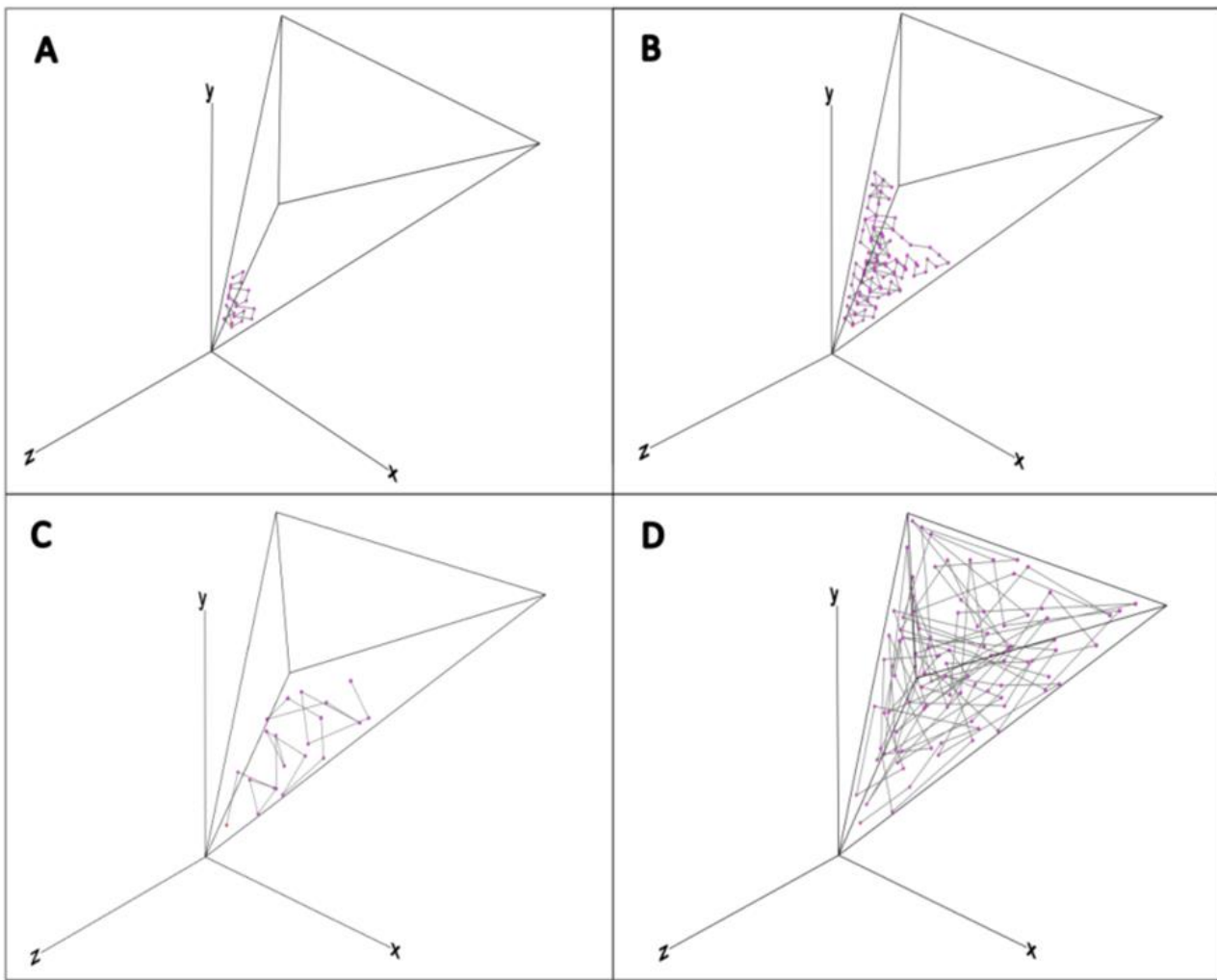


*Figure 12: Schematic of three-dimensional space and Markov Chain Monte Carlo (MCMC) sampler, showing how well the solution space can be sampled based on jump size and the number of iterations. The 'goal' is to sample the solution space adequately. (A) MCMC sampler with a small jump size, and a small number of iterations (B) MCMC sampler with a small jump size and a larger number of iterations (C) MCMC sampler with a larger jump size and a small number of iterations (D) MCMC sampler with a larger jump size and a larger number of iterations.*

### 4.3.2 LIM-MCMC Sampling Adequacy

There are no *a priori* tests to determine the sampling adequacy of the LIM-MCMC algorithm with the selected parameters. Instead, the performance of the LIM-MCMC algorithm (i.e., how well the solution space was sampled) is evaluated from the sampled solutions. In food web studies, the quality of the multiple plausible solutions has been evaluated by calculating the coefficient of variance (CoV) of each flow (mean of the flow divided by the standard deviation) to determine ‘convergence’ of each flow value mean and standard deviation (good CoV < 1) (Bell et al., 2017; de Jonge et al., 2020; Durden et al., 2017; van Oevelen et al., 2011). More broadly, model quality has been assessed as the convergence of the mean and standard deviations of each flow to a stable value (Saint-Béat et al., 2020, 2013; van der Heijden et al., 2020).

Markov Chain Monte Carlo (MCMC) convergence diagnostics may be more applicable to food web models but have yet to be incorporated in the broader ecological modelling research. The definition of the MCMC ‘convergence’ differs from the ‘convergence’ definition (CoV) previously used in food web studies. With MCMC convergence diagnostics, the solution space is considered well-sampled once the sampling chain posterior distribution  $P(x)$  approaches ‘convergence’ with the target distribution of the solution space  $Q(x)$  (Hogg and Foreman-Mackey, 2018; Mengersen et al., 1999; Roy, 2020; van Ravenzwaaij et al., 2018). MCMC convergence can be visually assessed via traceplots (Hogg and Foreman-Mackey, 2018; Roy, 2020; Van den Meersche et al., 2009), autocorrelation plots (Roy, 2020), and running mean plots (Roy, 2020; Saint-Béat et al., 2020, 2013). In addition to visual MCMC convergence diagnostics, a suite of convergence diagnostics are available to test various attributes of MCMC convergence (Plummer et al., 2020). No one convergence diagnostic is best, as each convergence diagnostic estimates convergence in a different method (Mengersen et al., 1999). Therefore, it is recommended that multiple convergence diagnostics are used to assess MCMC convergence (Hogg and Foreman-Mackey, 2018). For this study, future work includes using statistical MCMC convergence diagnostics to quantitatively determine how well the ensemble food web solutions represent the ecological constraints.

## 5 Conclusions

---

In this study, we found that ensemble network solutions that include the ecological variability of input data introduces uncertainty of ecosystem function in uMdloti Estuary, and therefore may offer more robust estimates of temporal ecosystem function in uMdloti Estuary than single solution networks. We found that ensemble solutions can detect shifts in ecosystem function after a disturbance event (mouth breach), which has potential ecosystem management relevance. From an ecosystem management perspective, more robust inferences of ecosystem status through ensemble methods, together with the advantage of statistical comparisons, may enhance data-driven decision making and contribute toward good ecosystem management practices. The next steps of this research are to investigate the communication of ensemble uncertainty in a practical and meaningful way for inclusion in ecosystem assessments and management. Through ensemble solutions, we determined that during drought conditions uMdloti Estuary ecosystem relies on primary producers rather than detritus to fuel the food web. The ecosystem further displays low cycling except immediately after a mouth breaching event and has higher metabolic activity during warmer summer months. When we consider these ecological interpretations together, we can infer that uMdloti ecosystem shows a decreased capacity to maintain system function during drought conditions and is therefore more vulnerable to further perturbations. We found that following a mouth breaching event the system responded by increasing overall cycling to potentially maintain its overall activity. At a nodal level, the recruitment of estuarine taxa into the estuary after the breach may have led to an increase in system cycling. Knowing which species are most involved in contributing energy flow and cycling should be a priority to maintain healthy ecosystem functioning. As ecosystem properties cannot be directly managed, connecting ecosystem-level information to nodal information can provide insight into how the system components (nodes) can be managed in a way to improve overall system function. The next steps of this research are to investigate how tangibly manageable system components, such as biomass, are connected to overall system function, and therefore which ecological indicators may be most meaningful to managers trying to maintain the flow of ecosystem services.

## References

---

- Borrett, S.R., 2013. Throughflow centrality is a global indicator of the functional importance of species in ecosystems. *Ecol. Indic.* 32, 182–196. <https://doi.org/10.1016/j.ecolind.2013.03.014>
- Borrett, S.R., Sheble, L., Moody, J., Anway, E.C., 2018. Bibliometric review of ecological network analysis: 2010–2016. *Ecol. Modell.* 382, 63–82. <https://doi.org/10.1016/j.ecolmodel.2018.04.020>
- Brooker, B., Scharler, U.M., 2020. The importance of climatic variability and human influence in driving aspects of temporarily open-closed estuaries. *Ecohydrology* 13, e2205. <https://doi.org/https://doi.org/10.1002/eco.2205>
- Chaalali, A., Saint-Béat, B., Lassalle, G., Le Loc'h, F., Tecchio, S., Safi, G., Savenkoff, C., Lobry, J., Niquil, N., 2015. A new modeling approach to define marine ecosystems food-web status with uncertainty assessment. *Prog. Oceanogr.* 135, 37–47. <https://doi.org/10.1016/J.POCEAN.2015.03.012>
- Chevillot, X., Tecchio, S., Chaalali, A., Lassalle, G., Selleslagh, J., Castelnau, G., David, V., Bachelet, G., Niquil, N., Sautour, B., Lobry, J., 2018. Global Changes Jeopardize the Trophic Carrying Capacity and Functioning of Estuarine Ecosystems. *Ecosystems*. <https://doi.org/10.1007/s10021-018-0282-9>
- Chrystal, R.A., Scharler, U.M., 2014. Network analysis indices reflect extreme hydrodynamic conditions in a shallow estuarine lake (Lake St Lucia), South Africa. *Ecol. Indic.* 38, 130–140. <https://doi.org/10.1016/j.ecolind.2013.10.025>
- Cliff, N., 1993. Dominance statistics: Ordinal analyses to answer ordinal questions. *Psychol. Bull.* 114, 494–509. <https://doi.org/10.1037/0033-2909.114.3.494>
- D'Alelio, D., Libralato, S., Wyatt, T., Ribera d'Alcalà, M., 2016. Ecological-network models link diversity, structure and function in the plankton food-web. *Sci. Rep.* 6, 21806.
- Day, J.W., Rybczyk, J.M., 2019. Chapter 36 - Global Change Impacts on the Future of Coastal Systems: Perverse Interactions Among Climate Change, Ecosystem Degradation, Energy Scarcity, and Population, in: Wolanski, E., Day, J.W., Elliott, M., Ramachandran, R.B.T.-C. and E. (Eds.), . Elsevier, pp. 621–639. <https://doi.org/https://doi.org/10.1016/B978-0-12-814003-1.00036-8>
- de Jonge, V.N., Schückel, U., 2021. A comprehensible short list of ecological network analysis indices to boost real ecosystem-based management and policy making. *Ocean Coast. Manag.* 208, 105582. <https://doi.org/10.1016/j.occoaman.2021.105582>
- de Jonge, V.N., Schückel, U., 2019. Exploring effects of dredging and organic waste on the functioning and the quantitative biomass structure of the Ems estuary food web by applying Input Method balancing in Ecological Network Analysis. *Ocean Coast. Manag.* 174, 38–55. <https://doi.org/10.1016/j.occoaman.2019.03.013>
- de Jonge, V.N., Schückel, U., Baird, D., 2019. Effects of spatial scale, species aggregation and balancing on carbon flows and ecological network analysis indicators of food webs. *Mar. Ecol. Prog. Ser.* 613, 15–47.
- de la Vega, C., Horn, S., Baird, D., Hines, D., Borrett, S., Jensen, L.F., Schwemmer, P., Asmus, R., Siebert, U., Asmus, H., 2018. Seasonal dynamics and functioning of the Sylt-Rømø Bight, northern Wadden Sea. *Estuar. Coast. Shelf Sci.* 203, 100–118. <https://doi.org/https://doi.org/10.1016/j.ecss.2018.01.021>
- Diffendorfer, J.E., Richards, P.M., Dalrymple, G.H., DeAngelis, D.L., 2001. Applying Linear Programming to estimate fluxes in ecosystems or food webs: an example from the herpetological assemblage of the freshwater Everglades. *Ecol. Modell.* 144, 99–120. [https://doi.org/https://doi.org/10.1016/S0304-3800\(01\)00342-8](https://doi.org/https://doi.org/10.1016/S0304-3800(01)00342-8)
- DWA, 2013. Classification of Water Resources and Determination of the Comprehensive Reserve and Resource Quality Objectives in the Mvoti to Umzimkulu Water Management Area: Volume 1: River Resource Quality Objectives.
- Fath, B.D., Asmus, H., Asmus, R., Baird, D., Borrett, S.R., de Jonge, V.N., Ludovisi, A., Niquil, N., Scharler, U.M., Schückel, U., Wolff, M., 2019. Ecological network analysis metrics: The need for an entire ecosystem approach in management and policy. *Ocean Coast. Manag.* 174, 1–14. <https://doi.org/10.1016/j.occoaman.2019.03.007>
- Fath, B.D., Scharler, U.M., Ulanowicz, R.E., Hannon, B., 2007. Ecological network analysis: network construction. *Ecol. Modell.* 208, 49–55. <https://doi.org/10.1016/J.ECOLMODEL.2007.04.029>
- Finn, J.T., 1980. Flow Analysis of Models of the Hubbard Brook Ecosystem. *Ecology* 61, 562–571. <https://doi.org/10.2307/1937422>
- Finn, J.T., 1976. Measures of ecosystem structure and function derived from analysis of flows. *J. Theor. Biol.* 56, 363–380. [https://doi.org/10.1016/S0022-5193\(76\)80080-X](https://doi.org/10.1016/S0022-5193(76)80080-X)
- Froneman, P.W., 2018. The Ecology and Food Web Dynamics of South African Intermittently Open Estuaries. IntechOpen, Rijeka, p. Ch. 5. <https://doi.org/10.5772/intechopen.72859>
- Gerber, G., Brooker, B., Scharler, U.M., n.d. autoLIM: an R package to automatically translate network data into LIM declaration file code.
- Guesnet, V., Lassalle, G., Chaalali, A., Kearney, K., Saint-Béat, B., Karimi, B., Grami, B., Tecchio, S., Niquil, N., Lobry, J., 2015. Incorporating food-web parameter uncertainty into Ecopath-derived ecological network indicators. *Ecol. Modell.* 313, 29–40. <https://doi.org/10.1016/j.ecolmodel.2015.05.036>
- Heymans, J.J., Ulanowicz, R.E., Bondavalli, C., 2002. Network analysis of the South Florida Everglades graminoid marshes and comparison with nearby cypress ecosystems, in: Ecological Modelling. pp. 5–23. [https://doi.org/10.1016/S0304-3800\(01\)00511-7](https://doi.org/10.1016/S0304-3800(01)00511-7)
- Hines, D.E., Ray, S., Borrett, S.R., 2018. Uncertainty analyses for Ecological Network Analysis enable stronger inferences. *Environ. Model. Softw.* 101, 117–127. <https://doi.org/10.1016/j.envsoft.2017.12.011>
- Jørgensen, S.E., Fath, B.D., 2006. Examination of ecological networks. *Ecol. Modell.* 196, 283–288. <https://doi.org/10.1016/J.ECOLMODEL.2006.02.029>
- Kones, J.K., Soetaert, K., van Oevelen, D., Owino, J.O., 2009. Are network indices robust indicators of food web functioning? A Monte Carlo approach. *Ecol. Modell.* 220, 370–382. <https://doi.org/https://doi.org/10.1016/j.ecolmodel.2008.10.012>
- Kones, J.K., Soetaert, K., van Oevelen, D., Owino, J.O., Mavuti, K., 2006. Gaining insight into food webs reconstructed by the inverse method. *J. Mar. Syst.* 60, 153–166. <https://doi.org/https://doi.org/10.1016/j.jmarsys.2005.12.002>
- Latham, L.G., 2006. Network flow analysis algorithms. *Ecol. Modell.* 192, 586–600. <https://doi.org/10.1016/j.ecolmodel.2005.07.029>
- Lau, M.K., Borrett, S.R., Hines, D.E., Singh, P., 2017. enaR: Tools for Ecological Network Analysis.
- Lawson, C.L., Hanson, R.J., 1995. Solving least squares problems. *Soc. Ind. Appl. Math.*
- Lawson, C.L., Hanson, R.J., 1974. Linear least squares with linear inequality constraints, Solving least squares problems.

- Le Guen, C., Tecchio, S., Dauvin, J.-C., De Roton, G., Lobry, J., Lepage, M., Morin, J., Lassalle, G., Raoux, A., Niquil, N., 2019. Assessing the ecological status of an estuarine ecosystem: linking biodiversity and food-web indicators. *Estuar. Coast. Shelf Sci.* 228, 106339. <https://doi.org/10.1016/J.ECSS.2019.106339>
- Leguerrier, D., Degré, D., Niquil, N., 2007. Network analysis and inter-ecosystem comparison of two intertidal mudflat food webs (Brouage Mudflat and Aiguillon Cove, SW France). *Estuar. Coast. Shelf Sci.* 74, 403–418. <https://doi.org/10.1016/j.ecss.2007.04.014>
- Macbeth, G., Razumiejczyk, E., Ledesma, R.D., 2011. Cliff's Delta Calculator: A non-parametric effect size program for two groups of observations. *Univ. Psychol.* 10, 545–555.
- Mahoney, P.C., Bishop, M.J., 2017. Assessing risk of estuarine ecosystem collapse. *Ocean Coast. Manag.* 140, 46–58. <https://doi.org/10.1016/j.ocecoaman.2017.02.021>
- Mukherjee, J., Karan, S., Chakrabarty, M., Banerjee, A., Rakshit, N., Ray, S., 2019. An approach towards quantification of ecosystem trophic status and health through ecological network analysis applied in Hooghly-Matla estuarine system, India. *Ecol. Indic.* 100, 55–68. <https://doi.org/10.1016/j.ecolind.2018.08.025>
- Nemeth, C., Fearnhead, P., 2021. Stochastic Gradient Markov Chain Monte Carlo. *J. Am. Stat. Assoc.* 116, 433–450. <https://doi.org/10.1080/01621459.2020.1847120>
- Niquil, N., Baeta, A., Marques, J.C., Chaalali, A., Lobry, J., Patrício, J., 2014. Reaction of an estuarine food web to disturbance: Lindeman's perspective. *Mar. Ecol. Prog. Ser.* 512, 141–154. <https://doi.org/10.3354/meps10885>
- Niquil, N., Jackson, G.A., Legendre, L., Delesalle, B., 1998. Inverse model analysis of the planktonic food web of Takapoto Atoll (French Polynesia). *Mar. Ecol. Prog. Ser.* 165, 17–29.
- Odum, E.P., 1985. Trends Expected in Stressed Ecosystems. *Bioscience* 35, 419–422. <https://doi.org/10.2307/1310021>
- Odum, E.P., 1969. The strategy of ecosystem development. *Science* (80-. ). 164, 262–270. <https://doi.org/10.1126/science.164.3877.262>
- Patten, B.C., 1995. Network integration of ecological extremal principles: exergy, emergy, power, ascendancy, and indirect effects. *Ecol. Modell.* 79, 75–84. [https://doi.org/10.1016/0304-3800\(94\)00037-I](https://doi.org/10.1016/0304-3800(94)00037-I)
- Pezy, J.-P., Raoux, A., Marmin, S., Balay, P., Dauvin, J.-C., 2018. What are the most suitable indices to detect the structural and functional changes of benthic community after a local and short-term disturbance? *Ecol. Indic.* 91, 232–240. <https://doi.org/https://doi.org/10.1016/j.ecolind.2018.04.009>
- Plummer, M., Best, N., Cowles, K., Vines, K., Sarkar, D., Bates, D., Almod, R., Magnusson, A., 2020. Package coda: Output Analysis and Diagnostics for MCMC.
- Poloczanska, E.S., Babcock, R.C., Butler, A., Hobday, A.J., Hoegh-Guldberg, O., Kunz, T.J., Matear, R., Milton, D., 2007. Climate change and Australian marine life.
- Robson, B.J., Arhonditsis, G.B., Baird, M.E., Brebion, J., Edwards, K.F., Geoffroy, L., Hébert, M.-P., van Dongen-Vogels, V., Jones, E.M., Kruk, C., Mongin, M., Shimoda, Y., Skerratt, J.H., Trevathan-Tackett, S.M., Wild-Allen, K., Kong, X., Steven, A., 2018. Towards evidence-based parameter values and priors for aquatic ecosystem modelling. *Environ. Model. Softw.* 100, 74–81. <https://doi.org/https://doi.org/10.1016/j.envsoft.2017.11.018>
- Roy, V., 2020. Convergence Diagnostics for Markov Chain Monte Carlo. *Annu. Rev. Stat. Its Appl.* 7, 387–412. <https://doi.org/10.1146/annurev-statistics-031219-041300>
- Safi, G., Giebels, D., Arroyo, N.L., Heymans, J.J., Preciado, I., Raoux, A., Schückel, U., Tecchio, S., de Jonge, V.N., Niquil, N., 2019. Vitamine ENA: A framework for the development of ecosystem-based indicators for decision makers. *Ocean Coast. Manag.* 174, 116–130. <https://doi.org/10.1016/j.ocecoaman.2019.03.005>
- Saint-Béat, B., Baird, D., Asmus, H., Asmus, R., Bacher, C., Pacella, S.R., Johnson, G.A., David, V., Vézina, A.F., Niquil, N., 2015. Trophic networks: How do theories link ecosystem structure and functioning to stability properties? A review. *Ecol. Indic.* 52, 458–471. <https://doi.org/10.1016/J.ECOLIND.2014.12.017>
- Saint-Béat, B., Fath, B.D., Aubry, C., Colombet, J., Dinasquet, J., Fortier, L., Galindo, V., Grondin, P.-L., Joux, F., Lalande, C., LeBlanc, M., Raimbault, P., Sime-Ngando, T., Tremblay, J.-E., Vaulot, D., Maps, F., Babin, M., 2020. Contrasting pelagic ecosystem functioning in eastern and western Baffin Bay revealed by trophic network modeling. *Elem. Sci. Anthr.* 8. <https://doi.org/10.1525/elementa.397>
- Saint-Béat, B., Vézina, A.F., Asmus, R., Asmus, H., Niquil, N., 2013. The mean function provides robustness to linear inverse modelling flow estimation in food webs: A comparison of functions derived from statistics and ecological theories. *Ecol. Modell.* 258, 53–64. <https://doi.org/https://doi.org/10.1016/j.ecolmodel.2013.01.023>
- Scharler, U.M., Baird, D., 2005. A comparison of selected ecosystem attributes of three South African estuaries with different freshwater inflow regimes, using network analysis. *J. Mar. Syst.* 56, 283–308. <https://doi.org/10.1016/j.jmarsys.2004.12.003>
- Scharler, U.M., Borrett, S.R., 2021. Network construction, evaluation and documentation: A guideline. *Environ. Model. Softw.* 140, 105020. <https://doi.org/https://doi.org/10.1016/j.envsoft.2021.105020>
- Scharler, U.M., Lechman, K., Radebe, T., Jerling, H.L., 2020. Effects of prolonged mouth closure in a temporarily open/closed estuary: a summary of the responses of invertebrate communities in the uMdloti Estuary, South Africa. *African J. Aquat. Sci.* 45, 121–130. <https://doi.org/10.2989/16085914.2019.1689911>
- Schückel, U., Kröncke, I., Baird, D., 2015. Linking long-term changes in trophic structure and function of an intertidal macrobenthic system to eutrophication and climate change using ecological network analysis. *Mar. Ecol. Prog. Ser.* 536, 25–38. <https://doi.org/10.3354/meps11391>
- Skowno, A.L., Poole, C.J., Raimondo, D.J., Sink, K.K., Van Deventer, H., Van Niekerk, L., Harris, L., Smith-Adao, L.B., Tolley, K.A., Zengeya, T.A., Foden, W.B., Midgley, G.F., Driver, A., 2019. National Biodiversity Assessment 2018: The status of South Africa's ecosystems and biodiversity. Synthesis Report. Pretoria, South Africa.
- Slinger, J.H., Taljaard, S., Largier, J.L., 2017. Modes of water renewal and flushing in a small intermittently closed estuary. *Estuar. Coast. Shelf Sci.* 196, 346–359. <https://doi.org/https://doi.org/10.1016/j.ecss.2017.07.002>
- Soetaert, K., van den Meersche, K., van Oevelen, D., 2009. limSolve: Solving Linear Inverse Models.
- Soetaert, K., van Oevelen, D., 2009. Modeling Food Web Interactions in Benthic Deep-Sea Ecosystems. *Oceanography* 22, 128–143.
- Tecchio, S., Chaalali, A., Raoux, A., Tous Rius, A., Lequesne, J., Girardin, V., Lassalle, G., Cachera, M., Riou, P., Lobry, J., Dauvin, J.C., Niquil, N., 2016. Evaluating ecosystem-level anthropogenic impacts in a stressed transitional environment: The case of the Seine estuary. *Ecol. Indic.* 61, 833–845. <https://doi.org/10.1016/j.ecolind.2015.10.036>
- Tecchio, S., Rius, A.T., Dauvin, J.C., Lobry, J., Lassalle, G., Morin, J., Bacq, N., Cachera, M., Chaalali, A., Villanueva, M.C., Niquil, N., 2015. The mosaic of habitats of the Seine estuary: Insights from food-web modelling and network analysis. *Ecol. Modell.* 312, 91–101. <https://doi.org/10.1016/j.ecolmodel.2015.05.026>
- Tomczak, M.T., Heymans, J.J., Yletyinen, J., Niiranen, S., Otto, S.A., Blenckner, T., 2013. Ecological Network Indicators of Ecosystem Status

- and Change in the Baltic Sea. PLoS One 8. <https://doi.org/10.1371/journal.pone.0075439>
- Ulanowicz, R.E., 2004. Quantitative methods for ecological network analysis. *Comput. Biol. Chem.* 28, 321–339. <https://doi.org/10.1016/j.combiolchem.2004.09.001>
- Ulanowicz, R.E., 1986. A Phenomenological Perspective of Ecological Development, in: Poston, T.M., Purdy, R. (Eds.), *Aquatic Toxicology and Environmental Fate: Ninth Volume*. ASTM International, West Conshohocken, PA, pp. 73–81. <https://doi.org/10.1520/STP29016S>
- Ulanowicz, R.E., Kay, J.J., 1991. A package for the analysis of ecosystem flow networks. *Environ. Softw.* 6, 131–142. [https://doi.org/10.1016/0266-9838\(91\)90024-K](https://doi.org/10.1016/0266-9838(91)90024-K)
- Van den Meersche, K., Soetaert, K., Oevelen, D. Van, 2009. xsample(): An R Function for Sampling Linear Inverse Problems. *J. Stat. Softw.* 30. <https://doi.org/10.18637/jss.v030.c01>
- Van Niekerk, L., Adams, A.B., Lamberth, S.J., Taljaard, S., MacKay, C.F., Bachoo, S., Parak, O., Murison, G., Weerts, S.P., 2019a. 'Chapter 6: Pressures on the Estuarine Realm', South African National Biodiversity Assessment 2018: Technical Report. Volume 3: Estuarine Realm. Pretoria, South Africa.
- Van Niekerk, L., Adams, J.B., James, N., Lamberth, S.J., MacKay, C.F., Turpie, J.K., Rajkaran, A., Weerts, S.P., Whitfield, A.K., 2019b. Chapter 3: A new Ecosystem Classification for South African estuaries, South African National Biodiversity Assessment 2018: Technical Report. Volume 3: Estuarine Realm. Report Number: SANBI/NAT/NBA2018/2019/Vol3/A. Pretoria, South Africa.
- Van Niekerk, L., Adams, J.B., Lamberth, S.J., MacKay, C.F., Taljaard, S., Turpie, J.K., Weerts, S.P., Raimondo, D., (eds), 2019c. South African National Biodiversity Assessment 2018: Technical Report. Volume 3: Estuarine Realm.
- van Oevelen, D., van den Meersche, K., Meysman, F.J.R., Soetaert, K., Middelburg, J.J., Vézina, A.F., 2010. Quantifying food web flows using linear inverse models. *Ecosystems* 13, 32–45. <https://doi.org/10.1007/s10021-009-9297-6>
- Vézina, A., Platt, T., 1988. Food web dynamics in the ocean. I. Best-estimates of flow networks using inverse methods. *Mar. Ecol. Prog. Ser.* 42, 269–287. <https://doi.org/10.3354/meps042269>
- Waspe, C., Mahabir, R., Scharler, U.M., 2018. FlowCAr: Flow Network Construction and Analysis.

# Supplementary Information 1

---

## nodeCycle.R

nodeCycle: calculate nodal cycling in one network

```
@author Gemma Gerber
@references Fath, B. D., Borrett, S. R. 2006. A Matlab function for Network Environ Analysis. Environ. Model. Softw. 21, 375-405.
@param x a network object. This includes all weighted flows into and out of each node.
@param zero.na LOGICAL: should NA values be converted to zeros?
@importFrom network get.vertex.attributes
@importFrom MASS ginv
@export nodeCycle
```

```
nodeCycle <- function(x, zero.na = TRUE) {
  Flow <- t(as.matrix(x, attrname = "flow"))
  "%v%" <- function(x, attrname) {
    network::get.vertex.attribute(x, attrname = attrname)
  }
  input <- x %v% "input"
  n <- nrow(Flow)
  I <- diag(1, nrow(Flow), ncol(Flow))
  T. <- apply(Flow, 1, sum) + input
  GP <- Flow / T.
  G <- t(t(Flow) / T.)

  if (zero.na) {
    GP[is.na(GP)] <- 0
    G[is.na(G)] <- 0
    GP[is.infinite(GP)] <- 0
    G[is.infinite(G)] <- 0
  } # zero.na = TRUE argument in enaFlow

  NP <- MASS::ginv((I - GP))
  rownames(NP) <- colnames(NP) <- colnames(GP)
  N <- MASS::ginv((I - G))
  rownames(N) <- colnames(N) <- colnames(G)
  tol <- 10
  N <- round(N, tol)
  p <- as.matrix(rep(1, n), nrow = n)
  dN <- diag(N)
  node_cycle <- ((dN - p) / dN * T.)
  rownames(node_cycle) <- rownames(Flow)
  node_cycle_return <- as.data.frame(t(node_cycle))
  node_cycle_return
}
```

## Supplementary Information 2

*Table SI2 1: Shapiro-Wilks test for normally distributed data, with **n** representing the number of samples, **W** is the Shapiro-Wilks statistics, and **p**-values indicate the probability of statistical significance (two-tailed). Statistical significance is indicated at levels < .001 (\*\*\*) , < .01 (\*\*) , and < .05 (\*).*

<b>Network Property</b>	<b>LDEI</b>			<b>LSEI</b>			<b>Central</b>			<b>Ensemble Median</b>		
	<b>n</b>	<b>W</b>	<b>p</b>	<b>n</b>	<b>W</b>	<b>p</b>	<b>n</b>	<b>W</b>	<b>p</b>	<b>n</b>	<b>W</b>	<b>p</b>
Detritivory: Herbivory Ratio (D:H)	13	0.771	< .01**	13	0.829	< .05*	13	0.694	< .001***	13	0.717	< .001***
Finn Cycling Index (FCI)	13	0.673	< .001***	13	0.752	< .01**	13	0.701	< .001***	13	0.683	< .001***
Total System Throughflow (TST <sub>flow</sub> )	13	0.972	0.916	13	0.94	0.454	13	0.94	0.451	13	0.944	0.506
Total System Cycling (TSTc)	13	0.711	< .001***	13	0.833	< .05*	13	0.703	< .001***	13	0.69	< .001***
log(D:H)	13	0.871	0.054	13	0.892	0.102	13	0.878	0.067	13	0.889	0.094
log (FCI)	13	0.967	0.854	13	0.905	0.156	13	0.954	0.662	13	0.953	0.637
log (TSTc)	13	0.95	0.595	13	0.929	0.332	13	0.919	0.243	13	0.917	0.226
Total Herbivory	13	0.939	0.438	13	0.944	0.515	13	0.953	0.644	13	0.957	0.712
Total Detritivory	13	0.891	0.101	13	0.859	< .05*	13	0.741	< .01**	13	0.802	< .01**
Total Net Primary Production	13	0.935	0.391	13	0.94	0.463	13	0.955	0.671	13	0.954	0.666
Primary Producer Sink	13	0.749	< .01**	13	0.953	0.646	13	0.946	0.543	13	0.943	0.494
log (Detritivory)	13	0.961	0.769	13	0.908	0.173	13	0.889	0.096	13	0.944	0.505
log (Primary Producer Sink)	13	0.973	0.923	13	0.947	0.555	13	0.9	0.135	13	0.942	0.489

## Supplementary Information 3

---

*Table SI3 1: Median flow values calculated from ensembles of 10,000 plausible food web solutions per month for uMdloti Estuary, compared to the flow values derived from the single network solutions Least Distance with Equalities and Inequalities (LDEI), Least Squares with Equalities and Inequalities (LSEI), and the central solution (Central).*

<b>Date</b>	<b>Total Net Primary Production (mgC·m<sup>-2</sup>·d<sup>-1</sup>)</b>				<b>Total Herbivory (mgC·m<sup>-2</sup>·d<sup>-1</sup>)</b>				<b>Total Detritivory (mgC·m<sup>-2</sup>·d<sup>-1</sup>)</b>				<b>Primary Producer Sink (mgC·m<sup>-2</sup>·d<sup>-1</sup>)</b>			
	<b>Ensemble Median</b>	<b>LDEI</b>	<b>LSEI</b>	<b>Central</b>	<b>Ensemble Median</b>	<b>LDEI</b>	<b>LSEI</b>	<b>Central</b>	<b>Ensemble Median</b>	<b>LDEI</b>	<b>LSEI</b>	<b>Central</b>	<b>Ensemble Median</b>	<b>LDEI</b>	<b>LSEI</b>	<b>Central</b>
Apr-15	367.70	275.89	259.04	370.69	432.75	297.48	276.26	424.27	333.57	65.74	75.95	63.00	99.63	24.65	34.46	29.92
May-15	355.49	278.72	261.06	79.36	404.57	296.72	278.94	88.74	288.59	78.44	92.54	267.47	78.98	22.80	33.72	279.13
Jun-15	162.23	133.31	123.23	128.96	191.45	140.50	131.95	168.49	220.31	31.35	35.77	30.31	50.25	14.59	20.52	70.05
Aug-15	116.43	64.94	62.17	38.88	160.91	68.55	64.18	41.25	209.65	54.38	57.56	91.51	44.63	15.40	15.38	26.37
Sep-15	323.07	164.93	156.18	116.61	394.06	174.14	159.50	120.15	456.10	227.05	239.49	362.14	30.25	3.14	6.81	8.92
Oct-15	277.44	206.99	196.34	252.93	348.14	216.54	210.37	262.50	303.38	66.09	91.16	169.08	85.94	16.36	27.71	52.08
Nov-15	253.68	250.04	239.49	25.97	316.84	267.76	260.10	55.69	247.89	69.85	110.44	220.66	126.62	20.40	36.80	389.68
Dec-15	307.10	329.02	304.73	443.15	360.44	343.02	332.54	456.51	279.81	68.36	85.68	166.17	150.84	37.04	51.65	49.78
Jan-16	408.40	469.46	439.27	626.36	470.52	486.69	474.76	647.50	303.28	65.00	87.95	172.17	197.03	70.08	92.83	149.78
Feb-16	687.74	557.42	531.41	694.14	743.05	577.61	563.01	836.15	497.88	198.20	227.00	181.88	79.31	51.76	74.13	17.88
Mar-16	636.96	480.77	460.93	419.08	704.04	524.96	470.99	459.61	505.03	301.20	329.78	509.90	118.31	34.72	42.31	51.72
Apr-16	503.79	436.57	412.04	477.07	577.69	465.05	437.56	582.48	320.04	90.73	115.01	91.56	192.10	47.46	69.54	139.72
Jun-16	206.41	191.99	179.20	262.97	274.55	209.37	191.83	312.73	214.26	42.12	52.99	39.78	149.16	29.48	37.98	44.53

Table SI3 2: Median ecological indicator values calculated from ensembles of 10,000 plausible food web solutions per month for uMdloti Estuary, compared to the flow values derived from the single network solutions Least Distance with Equalities and Inequalities (LDEI), Least Squares with Equalities and Inequalities (LSEI), and the central solution (Central).

Detritivory: Herbivory Ratio (D:H)					Finn Cycling Index (FCI) (%)				Total System Throughflow (TST <sub>flow</sub> ) (mgC·m <sup>-2</sup> ·d <sup>-1</sup> )			
Date	Ensemble Median	LDEI	LSEI	Central	Ensemble Median	LDEI	LSEI	Central	Ensemble Median	LDEI	LSEI	Central
Apr-15	0.77	0.22	0.27	0.15	6.08	0.05	0.05	0.01	1996.21	926.18	921.72	1184.73
May-15	0.67	0.26	0.33	3.01	5.01	0.05	0.05	0.09	1778.23	932.41	938.46	1248.46
Jun-15	1.09	0.22	0.27	0.18	6.30	0.06	0.05	0.01	1091.69	481.66	483.73	632.19
Aug-15	1.36	0.79	0.90	2.22	20.02	0.10	0.10	0.08	1014.10	310.35	311.09	357.48
Sep-15	1.17	1.30	1.50	3.01	16.17	0.26	0.26	0.30	2084.75	1099.06	1111.09	1349.29
Oct-15	0.76	0.31	0.43	0.64	7.50	0.08	0.07	0.04	1689.41	785.17	819.10	1120.48
Nov-15	0.78	0.26	0.42	3.96	3.53	0.03	0.03	0.08	1510.49	872.60	929.97	1412.15
Dec-15	0.74	0.20	0.26	0.36	3.37	0.01	0.01	0.01	1737.21	1062.12	1092.82	1452.96
Jan-16	0.66	0.13	0.19	0.27	4.68	0.02	0.02	0.00	2184.55	1561.69	1599.76	2043.51
Feb-16	0.64	0.34	0.40	0.22	9.29	0.08	0.07	0.08	3092.38	2029.91	2067.47	2308.05
Mar-16	0.73	0.57	0.70	1.11	5.74	0.07	0.07	0.05	3039.13	1982.57	1979.00	2499.90
Apr-16	0.54	0.20	0.26	0.16	3.21	0.03	0.02	0.01	2312.40	1415.04	1441.31	1705.99
Jun-16	0.78	0.20	0.28	0.13	4.34	0.02	0.02	0.02	1307.61	662.71	668.56	855.18

## Supplementary Information 4

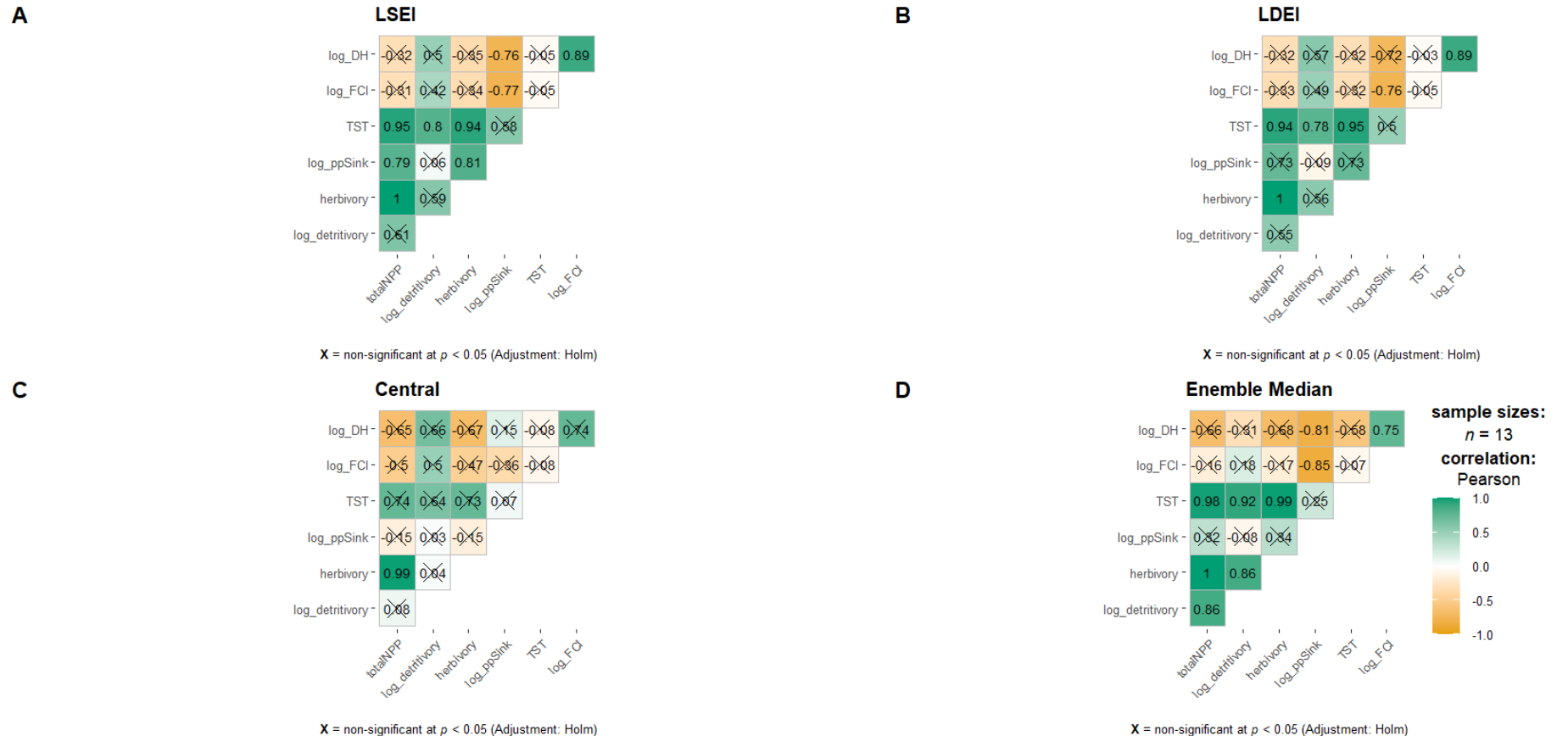


*Figure SI4 1: Correlation matrices showing Pearson correlation coefficients of relationships between ecological flows and indicators derived from uMdoti Estuary network single solutions A) Least Squares with Equalities and Inequalities (LSEI), B) Least Distance with Equalities and Inequalities (LDEI), C) Central solution, and D) ensemble medians. The crosses in each block indicate no statistical significance ( $p > .05$ , two-tailed).*